EXOENZYME DYNAMICS OF SURFACE OCEAN MICROBIAL COMMUNITIES IN RESPONSE TO OIL EXPOSURE

A Thesis

by

EMILY ANNE WHITAKER

Submitted to the Office of Graduate and Professional Studies of
Texas A&M University
in partial fulfillment of the requirements for the degree of

MASTER OF SCIENCE

Chair of Committee,	Jason Sylvan
Committee Members,	Antonietta Quigg
	Daniel Thornton
Head of Department,	Shari Yvon-Lewis

August 2018

Major Subject: Oceanography

ABSTRACT

Oil spills, while one of the most infamous manmade ecological disasters, remain relatively poorly understood, in particular the responses of microbial communities to the diverse suite of components in raw oil and chemical dispersants are just beginning to be elucidated. The 2010 Deepwater Horizon oil spill was historic in not only its volume and ecological damage, but also in the extent to which its progress and effects were monitored, particularly with respect to the microbial community. Analysis of exoenzymes can provide insight into how oil-degrading bacteria, as well as the bacterial community as a whole, respond to the changing chemical conditions experienced over the course of an oil spill. Using a multiscale approach with both mesocosms and three oil-degrading environmental isolates in culture, surface ocean microbes in oiled conditions were shown to be highly active with respect to ß-glucosidase, leucine aminopeptidase, and alkaline phosphatase. The activities measured in the mesocosms are some of the highest reported for environmental systems in the literature. Additionally, both coastal and open ocean microbial communities in mesocosms and all three isolates in bottle experiments demonstrated the ability to significantly modify their alkaline phosphatase and ß-glucosidase kinetics over just a few days in culture. Exposure to oil tended to change the patterns in enzyme activity over the course of each experiment. In the mesocosm experiments, differences in enzyme activity between the offshore community and the coastal community were greater than the differences between the control and oil treatments, indicating source microbial community composition has a greater impact than exposure to oil for enzyme activity. Supporting this hypothesis, there was as much variability in activity for alkaline phosphatase and leucine

aminopeptidase between the three oil-degrading strains, as between the two mesocosm experiments. In general, the mesocosms had higher V_{max} and lower K_m values for each enzyme than any of the strains, though for alkaline phosphatase and leucine aminopeptidase the strains showed as much diversity in terms of kinetic values as the mesocosms.

DEDICATION

To my family.

ACKNOWLEDGEMENTS

I would like to thank my advisor and thesis chair Dr. Jason Sylvan for his guidance and direction through this thesis project, as well as through three total months of mesocosm experiments, one drilling expedition on the other side of the world, one rapid-response cruise, two crises of career direction, three years of life in Texas, and no fewer than six separate projects. I would additionally like to thank my committee members Dr. Daniel Thornton and Dr. Antonietta Quigg for their direction and perspective on this thesis, as well as Dr. Quigg's fearless leadership of the ADDOMEx consortium.

CONTRIBUTORS AND FUNDING SOURCES

This work was supported by a thesis committee consisting of Professors Jason Sylvan, advisor, and Daniel Thornton of the Department of Oceanography and Professor Antonietta Quigg of the Department of Marine Biology at Texas A&M Galveston.

The microbial isolates used in this study were provided by Dr. Manoj Kamalanathan and Dr. Hernando Bacosa at Texas A&M Galveston. All other work conducted for this thesis was completed by the student independently.

This research was supported by a grant from The Gulf of Mexico Research Initiative to support consortium research entitled ADDOMEx (Aggregation and Degradation of Dispersants and Oil by Microbial Exopolymers) Consortium.

TABLE OF CONTENTS

Page

LIST OF FIGURES

Page

LIST OF TABLES

Page

1. INTRODUCTION

1.1 Background

Microbial communities and consortia are important mediators of the biodegradation of oil in the aftermath of spills in ocean environments (Silliman et al., 2012, Quigg et al., 2016, García et al., 2009, Joye et al., 2011, Seidel et al., 2016, Miralles et al., 2007, Atlas, 1981, Wang et al., 2016, Arnosti et al., 2014). While observational and quantitative data exist for several historic oil spills, relatively recent advances in genomic sequencing technology and high-resolution chemical analyses permitted a far more rapid and microbially-focused research response to the 2010 Deepwater Horizon oil spill in the Gulf of Mexico (Ziervogel et al., 2012, Hu et al., 2017, Edwards et al., 2011, Liu et al., 2012, Passow et al., 2012, Wade et al., 2016, Nie et al., 2016). For more than four months during the spring and summer of 2010, a damaged blowout preventer on the wellhead of the oil drilling rig Deepwater Horizon released ~5 million barrels of Macondo crude oil from the seafloor at 1522 m depth in the Northern Gulf of Mexico (McNutt et al., 2012, Joye et al., 2011). Most of this oil (~60%,) rose to the ocean surface where the volatile phases evaporated and the rest formed slicks, dissolved into the surface waters, sorbed to marine particles, or could not be unaccounted for (Joye et al., 2011). Responders throughout the course of the spill attempted to minimize the surface slicks using the dispersant Corexit 9500 and others to locally increase the solubility of hydrocarbons into the water. Even though the wellhead was sealed in September 2010, the released oil persisted in the water column, eventually becoming buried in ocean sediments and working its way deep onto beaches and up estuaries in the following months and years (Daly et al., 2016, Romero et al., 2015, Silliman et al., 2012, Turner et al., 2016, Yan et al., 2016, Pallardy, 2015).

Though research is ongoing, the current consensus is the DWH oil spill caused a massive biological reaction from the microbial communities of the Gulf, from benthic forams to phytoplankton and native hydrocarbon degrading bacteria (Edwards et al., 2011, Hastings et al., 2014, Kim et al., 2015, Passow et al., 2012, Shiller and Joung, 2012, Silliman et al., 2012, Turner et al., 2016, Ziervogel et al., 2012). The order of events and responses upon exposure to oil, and the effects remediation efforts ultimately had on rates of biodegradation remain areas of active research. This ongoing work has found successional patterns of microbial communities during the spill, begun to link community make-up to oil-degrading functions in different environments, and has tracked the oil through the ocean food web (Doyle et al., 2018, Quigg et al., 2016, Passow et al., 2012, Kim et al., 2015, Chanton et al., 2012, Ziervogel et al., 2012). However, a fundamental unknown in this puzzle is the nutritional state of the microbial community before, during, and after the spill. Measurements of nutrients during the spill or respiration rates alone cannot show limitation of the growth of the microbial community with respect to phosphorus, nitrogen, or even carbon. Nitrogen and phosphorus have been shown to be limiting nutrient(s) in the region of the Louisiana Shelf where the spill occurred (Sylvan et al., 2006), though it is not yet known if this was a factor in how the surface microbial community responded to oil, or what would be the effects of amending the system with nutrients, as has been proposed from previous oil spills (Miralles et al., 2007, Patton et al., 1981).

Exoenzyme measurements present a comprehensive way to understanding the metabolic needs of the microbial community as a whole. Microbes use exoenzymes to degrade molecules too large to incorporate as is into the cell, and therefore analysis of community exoenzyme activity can inform us about nutritional needs within a microbial community, including in

response to environmental perturbations such as an oil spill. In addition, high levels of exoenzyme activity have previously been associated with highly active microbial communities, particularly those associated with marine-oil snow particles (Daly et al., 2016, Vetter and Deming, 1999, Arnosti et al., 2014, Ziervogel et al., 2012). Exoenzyme analysis was used here to analyze the response of whole microbial communities in mesocosm experiments and individual oil-degrading isolates in bottle experiments to exposure to oil or oil plus chemical dispersant.

1.2 Exoenzymes in aquatic environments

Exoenzymes are responsible for breaking down large polymers, larger than approximately 60kDa (Weiss et al., 1991), that cannot be transported into the cell into monomers that can pass through the cell wall . Critically, exoenzymes are responsible for the rapid conversion of particulate organic matter to dissolved organic matter (Amon and Benner, 1994, Azúa et al., 2003, Baines and Pace, 1991, Biddanda and Benner, 1997, Kawasaki and Benner, 2006), a process observed in marine snow particles, where high environmental rates of exoenzyme activity occur (Martinez et al., 1996, Smith et al., 1992, Alderkamp et al., 2007, Vetter and Deming, 1999). Exoenzymes are produced as scavengers of organic matter, frequently when the cell is lacking in the product of the molecule cleaved by the enzyme (Chróst and Rai, 1993, Allison, 2005, Christian and Karl, 1995, Fabiano and Danovaro, 1998, Hoppe et al., 1988). The highest rates of exoenzyme production occur in response to deficiency in the product of the reaction catalyzed by the enzyme (Hoppe, 1991, Sinsabaugh and Follstad Shah, 2012). Therefore, measuring exoenzyme parameters such as their activities, kinetics properties, and ratios thus gives insight into the nutritional states of the microbial community. Utilizing this approach to exoenzymes in a mesocosm setting allows for tracking of the nutritional metabolic

requirements of the microbial community over the course of a simulated environmental condition, including a simulated oiled system (Arnosti et al., 2011, Chróst and Rai, 1993, Murray et al., 2007, Van Wambeke et al., 2016). The same approach can be used with individual microbial species or isolates to determine how well whole-community responses represent the sum of their individual species.

1.3 Properties of exoenzymes

1.3.1 Exoenzyme activity

The three most commonly assayed enzymes assayed in ecological studies representative of carbon, nitrogen, and phosphorus demands are, respectively, β-glucosidase (BG), leucine aminopeptidase (LAP), and alkaline phosphatase (AP) (Sinsabaugh and Follstad Shah, 2012, Arnosti, 2011, Marx et al., 2005, Murray et al., 2007). BG is a general indicator of heterotrophic activity as it cleaves glucose from the terminal ends of long storage and structural polysaccharides. LAP is associated with organic nitrogen via cleavage of amino acids from polypeptides and is thus tied to N acquisition. Finally, AP cleaves inorganic phosphate from organophosphate ester compounds and is primarily expressed under conditions of high inorganic phosphorus demand relative to availability. These activities all individually inform on the metabolic activities and demands of the microbial community, but comparing these representative enzymes of C, N, and P demand to each other over time brings additional insight (Sinsabaugh and Follstad Shah, 2012, Ammerman and Glover, 2000).

1.3.2 Exoenzyme kinetics

The kinetic properties of exoenzymes are useful for comparing the ecological strategies of microbial communities across different environments (Alderkamp et al., 2007, Martinez et al.,

1996, Marx et al., 2005, Zimmerman et al., 2013). The diagnostic parameters for enzymes are the maximum velocity, V_{max}, and the half saturation constant, K_m (Fig. 1).

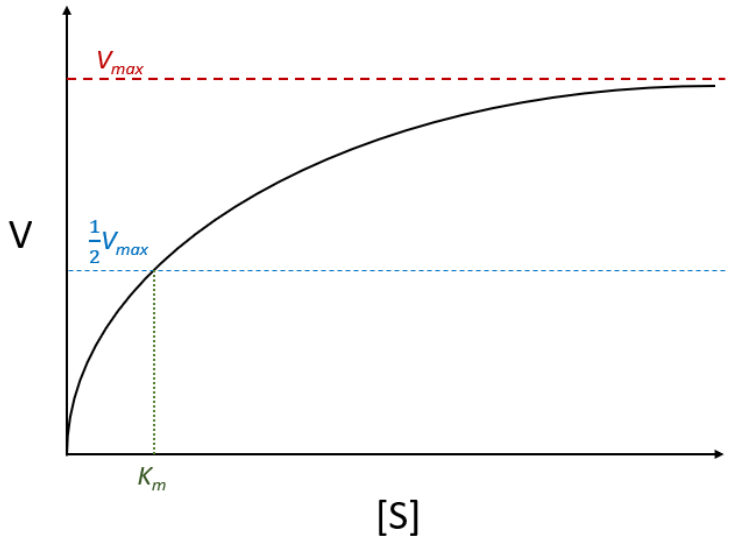

Figure 1. Relationship between kinetic parameters Vmax and Km

The maximum velocity is a theoretical rate at which the enzyme would act in the presence of infinite substrate. In practice, V_{max} occurs whenever the substrate concentrations are significantly larger than K_m. The half saturation constant is the substrate concentration at which enzyme activity rate is half of V_{max}. Conceptually, K_m can be understood as the sensitivity of enzymes to low substrate concentrations, with a low K_m implying that the enzyme can reach high relative activities, even when the substrate concentration is low (Azam and Hodson, 1981). However, K_m on its own only functions as a measure of sensitivity for idealized single-substrate enzyme kinetics (Marx et al., 2005). BG, LAP and AP all hydrolyze multiple substrates, and therefore interpreting K_m alone as a measure of enzyme sensitivity to its substrate must done with care and is dependent on the system being studied. LAP is particularly well known for its

non-specificity not just for substrates but also in its products, as it can cleave a suite of terminal amino acids such as methionine and alanine, in addition to leucine (Martinez and Azam, 1993, Steen et al., 2015). In such situations, a better, more universally comparable estimation of enzyme sensitivity is the initial slope of the kinetic curve. This is the range of substrate concentrations where the concentration of enzyme far outweighs the substrates, so the rate is limited by the kinetic parameters of the enzyme. Thus when [S] << K_m, the Michaelis-Menten equation simplifies to a linear relationship between V_{max}/K_m and the substrate concentration (Hoppe et al., 1988, Lancelot, 1979). This is a powerful tool because V_{max}/K_m can be estimated for all samples regardless of the substrate saturation state reached in the kinetic experiment (Baltar et al., 2009).

Often there is a tradeoff between the substrate sensitivity of the enzyme and its maximum rate of activity, i.e. between K_m and V_{max}. Thus, enzymes with low K_m typically can function efficiently even at low substrate concentrations, but when substrate concentration is high they can be outcompeted by other enzymes that do not respond to low substrate concentrations but have a higher V_{max}. This is an example of niche partitioning within enzymes as low K_m and V_{max} are specialized for low substrate availability and high K_m and V_{max} for high substrate availability (Alderkamp et al., 2007, Chróst and Overbeck, 1987, Marx et al., 2005, Sebastián et al., 2004b). Niche partitioning between enzymes does not necessarily translate to metabolic niche partitioning between microbes, although it certainly can (Walker et al., 2010), or even community composition shifts because a single organism can possess several types of a single enzyme. K_m and V_{max} comparisons, however, are used to detect shifts in the dominant form of a specific enzyme, or isozyme, expressed in a community. Changes in K_m and V_{max} represent

different nutrient acquisition strategies reflecting different substrate conditions across environments, making their analysis particularly useful for tracking microbial communities and strains growing with or without oil (Alderkamp et al., 2007, Sinsabaugh and Follstad Shah, 2012, Marx et al., 2005, Arnosti et al., 2014, Ziervogel et al., 2014).

1.3.3 Enzyme repression

Alkaline phosphatase is widely distributed taxonomically and is one of the most highly expressed enzymes in the environment (Sinsabaugh and Follstad Shah, 2012). Much of the early environmental work with AP affirmed the original model of increased expression with low phosphate availability, and decreased or repressed activity when phosphate was replete (Chróst and Overbeck, 1987, Chróst and Rai, 1993). However, demonstration of AP activity does not imply a direct relationship with local phosphate levels, or even with phosphate acquisition (Sebastián et al., 2004a). Expression may be constitutive, such as in some coastal aquatic environments with relatively high AP activities despite high dissolved inorganic phosphate concentrations (Davis and Mahaffey, 2017). AP expression has also been shown to be phosphate insensitive, not due to constitutive expression, but rather as a means of acquiring reduced carbon in energy limited environments (Baltar et al., 2009, Bergauer et al., 2018). Repression experiments attempt to investigate the reason an enzyme is expressed through addition of the hypothesized end product (Albertson et al., 1990, Davis and Mahaffey, 2017). For example, if AP activity is used primarily for acquiring phosphate in an experimental system, then AP activity should decrease upon the addition of phosphate. However, if enzyme activity remains unchanged, then AP is not phosphate-repressible and the system may be tested for catabolite or carbon limitation by adding a readily metabolizable carbon substrate, depending on the system.

Attempting to repress AP activity with both phosphate and a simple catabolite such as glucose can then help determine which of the two may be limiting in an environment.

1.4 Exoenzymes in communities and in strains

Combining measurements of overall activities over time, kinetic parameters, and repression experiments of key exoenzymes in a mesocosm setting allows for the tracking of community nutrient and metabolic requirements over the course of a simulated oil spill. The approach has inter-domain community complexity, which allows for conclusions drawn to be extrapolated to natural systems. However, it can also lead to difficulty determining the impacts of specific community members, or groups of community members, like hydrocarbon degraders in an oil spill simulation, within the signal from the entire microbial community. Like every environmental study, this runs into the classic trade off of specificity of results versus applicability to natural systems. Mesocosm experiments bring realism, but it is difficult to interpret enzyme measurements such as "community kinetics" and community activity, when in reality one is measuring the integrated kinetics and activities of all present isozymes and possibly other enzymes not even targeted with the fluorogenic substrates. Single-strain cultures of oil-degrading bacteria found in the mesocosms can bring some much-needed conceptual precision to the community activities. While monocultures have limited direct applicability to more complex oiled systems, they are essential for understanding what single strains can bring to the community table through their enzymatic function. Measuring how kinetic parameters, overall activities, and repressibility vary over time and oil exposure in several oil-degrading strains gives important context for what the oil-degraders in the mesocosms may contribute to community enzyme measurements. Ultimately the combination of the complementary limitations and

strengths of community-based and single strain approaches can help reveal the changing metabolic conditions and responses of surface ocean communities in oil spills.

1.5 Hypotheses

The offshore and coastal communities in the mesocosms are from different nutrient regimes, and their exoenzymes are likely optimized accordingly. I predict that the offshore community will have lower Vmax and Km values than the coastal community for each treatment.

Each of the three hydrocarbon degrading strains likely does not degrade the same fraction of crude oil, or at the same rate. Thus I predict that they will have distinct nutrient demands when growing on oil, which will be reflected as different patterns in exoenzyme activity over time as well as distinct kinetic parameters for each enzyme.

As likely members of the mesocosm communities, I predict that the three strains will have activities in the same range as the mesocosms for each measured enzyme, as well as kinetic parameters within the range of the mesocosms. Additionally, I predict that as more complex systems comprised of many strains with presumably many isozymes, the mesocosms will have a larger range of kinetic parameters than the three strains.

1.6 Objectives

To investigate these hypotheses this study will:

1. Use mesocosm experiments to examine the effects of both oil and microbial community source on community exoenzyme activity and kinetic properties.

2. Parameterize and add context to the mesocosm results by using three oil-degrading strains isolated from a mesocosm will be assayed for exoenzyme activities, kinetic properties, and repressibility for the purpose of constraining the potential effects of individual strains on community exoenzyme measurements.

2. METHODS

2.1 Mesocosm setup and sampling

To replicate the conditions of an oil spill, two separate mesocosm experiments were conducted during July 2016 using different source water to reflect two different regions of the northern Gulf of Mexico (GoM) affected by the 2010 BP Deepwater Horizon blowout, one on the continental shelf at 29°22N, 93°23W and one offshore near the Flower Gardens Bank National Marine Sanctuary at 27°53N, 94°2W, reflective of open ocean microbial communities (Fig. 1). The source water formed the base for four different experimental treatments: no oil added (Control), the water-accommodated fraction of Macondo Surrogate crude oil in seawater (WAF), oil added to the water-accommodated fraction with the chemical dispersant Corexit 9500 (CEWAF), and CEWAF diluted to the same concentration of oil as the WAF treatment (DCEWAF) (Wade et al., 2017).

The offshore experiment was run for 96 hours (11-15 July, 2016), and the coastal experiment for 72 hours (18-21 July, 2016). Starting at time point zero, and then every twelve hours after through the end of the experiment, each mesocosm tank was sampled via a twist-stoppered spigot near the bottom of each tank into clean, opaque Nalgene bottles. Cell count samples (10mL) were fixed with 2% final concentration formalin and stored at 2˚C until further processing. All samples (15mL) for exoenzyme analyses were aliquoted into sterile falcon tubes and incubations were begun immediately. BG, LAP, and AP were measured at each time point according to the methods detailed below. Kinetics for each enzyme were determined at the beginning of each mesocosm and repression experiments were conducted at the final time point.

Figure 2. Map of source water locations for mesocosms

2.2 Isolate descriptions

Three strains of bacteria, initially named C8, C12 and W14, were isolated from a subsequent mesocosm experiment during summer 2017 and used for isolate experiments (H. Bacosa, pers. comm.). These strains were cultured on agar plates supplemented with Corexit9500, and demonstrated abilities to degrade both Corexit9500 and crude oil. 16S rRNA sequencing of the strains revealed them to belong to *Thalassospira* (str. C8), *Aestuariibacter* (str. C12), and *Alteromonas* (str. W14) respectively, most closely matching genbank entries KC238399.1, MF070532.1, and MF359338.1 (Fig. 2). Preliminary experiments using the same media detailed below, found that all three strains express AP and LAP under experimental conditions, while only *Alteromonas* str. W14 expresses BG under the same conditions.

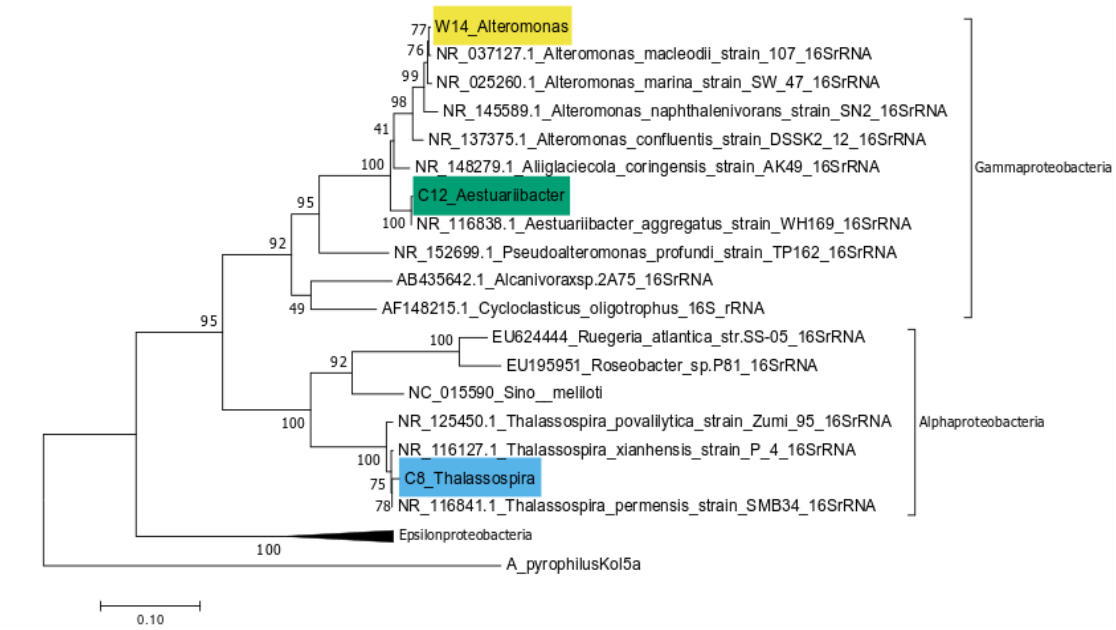

Figure 3. Maximum likelihood tree of the three isolates, 500 bootstrap iterations.

2.3 Monoculture setup and sampling

Thalassospira str. C8, *Aestuariibacter* str. C12, and *Alteromonas* str. W14 were grown in triplicate 1L incubations in both control seawater and oil amended seawater (WAF). Seawater collected near Galveston, TX, amended with f/2 nutrients formed the base of both treatments: seawater (Control) and WAF. The monoculture experiments required sterile media thus the base seawater was 0.2µm filtered then autoclaved, and the WAF-making protocol was modified from that used for the mesocosms (Wade et al., 2017) to include 0.2µm filtration of the oil before use. All strains were cultured to high biomass in nutrient broth media in preparation for starting monoculture incubations. Aliquots of starter culture were pelleted and washed with control media before resuspension and addition to experimental incubations at an approximate starting density of 10^6 cells/mL and a total added volume of less than 10mL per bottle.

Samples for cell counts were taken and fixed with final concentration 2% formalin and stored at 2°C immediately after starting the cultures and every 24 hours thereafter. Cultures were maintained at 18°C on a 12-hour light/dark cycle while being stirred at ~300rpm on magnetic stir plates. Sampling for kinetic curves occurred on odd days after the cultures were started and sampling for repression experiments occurred on even days. Each 10mL sample for exoenzyme analysis was transferred under aseptic conditions from the culture flask via 15mL pipettor to a clean 15mL falcon tube for immediate analysis. Cultures were maintained for a total of six days after inoculation. Experiments occurred over the course of two weeks; *Thalassospira* str. C8 and *Aestuariibacter* str. C12 were grown and analyzed simultaneously during the first week (15-21 January 2018) and *Alteromonas* str. W14 the second week (22-28 January 2018).

2.4 Measuring Exoenzyme activity

Enzyme activity was measured using small molecule substrate analogues that become fluorescent after they are cleaved by an enzyme (Hoppe, 1991). Assays for both BG and AP used the fluorescent molecule 4-methyumbelliferone bound to a glucose or phosphate group as MUF-G and MUF-P, respectively. Assays for LAP used 7-amino-4-methylcoumarin bound to a leucine group as Leucine-AMC. For the mesocosm experiments, BG assays were run at 200μM concentration MUF-G, AP at 150μM MUF-P, and LAP at 400μM Leucine-AMC. All activity measurements were conducted in 15mL dark incubations maintained at ambient temperature and shaken before sampling for fluorescence. Triplicate 200uL aliquots were sampled from each 15mL incubation into a 96-well plate. Each well received 67uL of 50mM pH 10.8 borate buffer to increase and normalize sample pH. Fluorescence was immediately measured by a Tecan Spark 10M multimode microplate reader at excitation-emission wavelengths of 365 and 455nm

respectively. Each 96-well plate contained duplicate standard curves and blanks for both MUF and AMC. Fluorescence was measured at three time points ranging from 15 minutes to 2 hours depending on the predicted rate of increase and the physical limitations of pipetting. Activity was measured as the slope of the linear equation fit via least squares to the sample fluorescence over time.

2.5 Kinetic parameter measurements

Kinetics curves were constructed by measuring enzyme activity at five different substrate concentrations from <1uM to a maximum concentration greater than the expected saturation point for each enzyme. For the monocultures, substrate concentrations ranged from 1 to 500μM, 1 to 1000μM, and 0.1 to 100μM respectively for AP, LAP, and BG. For the mesocosms, substrate concentrations ranged from 1 to 400μM for AP and LAP, and 0.2 to 40μM for BG. A two-parameter Michaelis-Menten equation (Eqn. 1) was fit to the curve formed by the activities measured at each substrate concentration using the R package drc (Ritz et al., 2016).

$$Equation\ 1.\quad V = \frac{V_{max} \times S}{K_m + S}$$

In cases where even the highest concentration of substrate was not saturating, non-linear curve fitting did not result in a convergent solution for K_m or V_{max}. Alternatively, the solution did converge, but the standard errors on the estimated parameters were greater than the parameters themselves. Thus, in order for K_m and V_{max} to be estimated *individually*, the kinetic curve must have approached saturation within the measured substrate concentrations. However, these cases reasonably fulfill the assumption of $S << Km$, which allows for the simplification of Equation 1

to a linear equation where the measured activity is a function of *S* where the slope is defined by the proportion of V_{max} to K_m (Eqn. 2).

$$Equation\ 2.\ \ V = \frac{SV_{max}}{K_m}$$

Fitting a linear equation to the non-convergent kinetic curve allows for the estimation of Vmax and Km relative to each other, but not individually as is the case for convergent samples. For comparison purposes, V_{max}/K_m was calculated for the convergent samples using the parameter estimates from the fitted Michaelis-Menten equation. This parameter is referred to in this work as enzyme sensitivity, as it is a measure of the response rate of an enzyme to its substrate (Baltar et al., 2009). Note that V_{max}/K_m has units of inverse time, which defines it as a true rate and therefore independent of population size.

2.6 Repression experiments

For each monoculture strain, AP activity was measured in the presence of three concentrations of a single repressor: phosphate at 100 μM, 1000 μM, and 10mM, and glucose at 10, 100, and 1000 μM. After subsampling from the ongoing monoculture experiments, the repressor was immediately added to each tube and then incubated at room temperature in the dark for 1-2 hours to allow for repression before the addition of MUP and subsequent fluorescence measurements. Relative repression was calculated using the activity in the highest concentration of repressor normalized for each experiment by the estimation of unrepressed activity V_0. The unrepressed activity was estimated as the y-intercept from a simple linear regression of activity over substrate concentration.

$$Relative\ Repression = \frac{V_0 - V_{rep}}{V_0}$$

This normalization results in values of relative repression ranging from full repression at 1 and no repression at 0. Note that the results have the potential to be <0, i.e. “negative repression”, which indicates an increase in activity in the presence of the repressor.

2.7 Total cell abundance

Total cell abundance was determined for the mesocosms through direct cell counts for each experimental tank at each mesocosm time point. Fixed cells were first stained with 45μM DAPI for five minutes in the dark before vacuum filtering onto 0.2μm black polycarbonate filters. Filters were then mounted on glass slides, preserved with two drops of antifade solution (90 mM p-phenylenediamine and 45% glycerol dissolved in phosphate buffered saline, filter sterilized), sealed with a glass coverslip, then stored at -20°C until they were counted. Slides were counted on an epifluorescence microscope (Zeiss Axio Imager.M2) using a 100μm x 100μm ocular counting grid at 1000x magnification. Total cell abundance was determined using at least 10 fields of view and 200 cells per slide.

3. RESULTS

3.1 Mesocosm activities

LAP activities were relatively comparable between the offshore and coastal mesocosms, with each treatment having similar ranges of activity (Table 1.). Maximum observed activities ranged from 1350-7800 nM/h, but between the mesocosms the difference between the same treatments in the coastal and offshore experiments was 1.8-fold or less. There was no pattern in maximum activity between the two experiments except that maximum activity in CEWAF was 3.2 to 5.8-fold higher than the other treatments. However, the minimum LAP activities were always lower in the offshore mesocosms than the coastal, with a range of 1.1 to 2.4-fold less. This difference in minimum activities is most strongly observed in the control and WAF treatments where the minimum coastal LAP activity is 2.4-fold higher than that of the offshore.

Table 1. Maximum and minimum observed LAP activities of the coastal and offshore mesocosms. Activities are in nM/h.

Mesocosm	Treatment	Minimum LAP Activity	Minimum SE	Maximum LAP Activity	Maximum SE
Offshore	Control	185	5	1620	35
Coastal	Control	350	50	2110	580
Offshore	WAF	170	25	1900	75
Coastal	WAF	400	30	1350	265
Offshore	CEWAF	810	5	7800	515
Coastal	CEWAF	1200	65	7720	2530
Offshore	DCEWAF	250	15	2450	115
Coastal	DCEWAF	280	2	1340	75

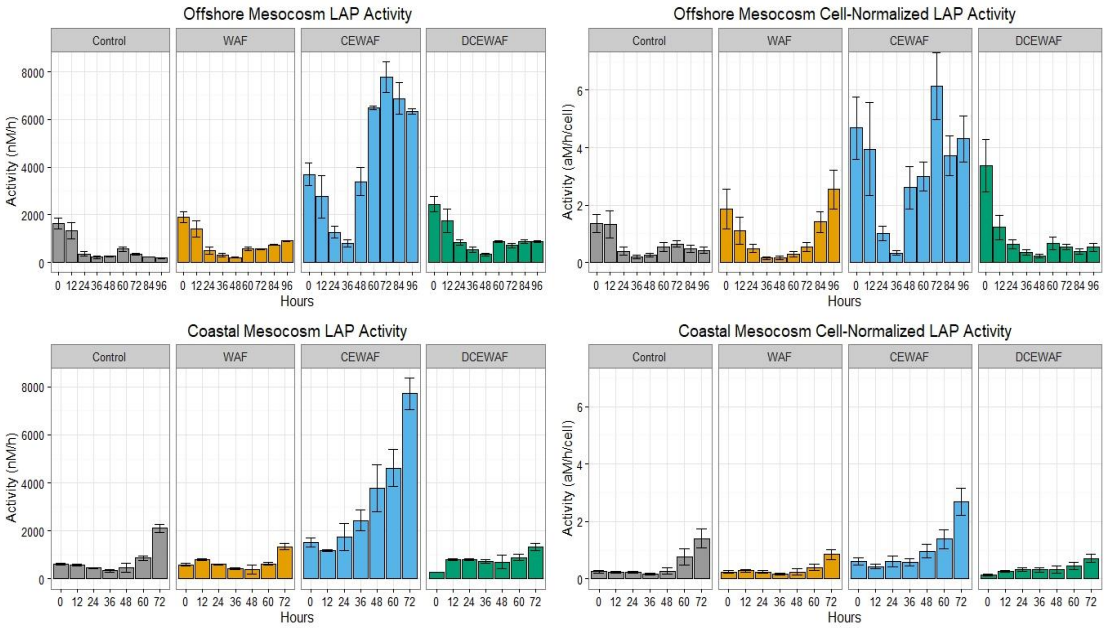

Figure 4. Coastal and offshore mesocosms LAP activity time series. LAP activities measured every 12 hours in offshore and coastal mesocosms. Activities are measured in nM MUF produced per hour while cell-normalized activities are in attaM per hour per c

Though the ranges of LAP activity were similar between the offshore and coastal mesocosms, the patterns in activity over the course of the experiment were largely opposite each other. Specifically, LAP activities decreased over time in the control, WAF, and DCEWAF treatments in the offshore experiment and increased over time in the coastal experiment (Fig. 3). As with many of the measured enzyme parameters, LAP activities in CEWAF treatments were the highest in both experiments (Table 1); the changes through time were variable, but LAP was significantly higher at the end of each experiment (offshore $p = 0.0023$, coastal $p = 0.035$). In all cases, CEWAF appears to be a more extreme version of the pattern observed in the other treatments in their respective mesocosms. In the offshore mesocosm during hours 0-36, where the other three treatments see a sharp decrease in

activity, CEWAF does as well. Additionally, where WAF and DCEWAF exhibit a slight increase in activity after hour 48, CEWAF shows a dramatic increase in activity 12 hours earlier. Likewise, in the coastal mesocosms where the three other treatments show either constant or very slightly increasing activity until the final time point, CEWAF shows an almost exponential increase in activity over the whole time-course of the experiment.

Cell normalization results in higher activities in the offshore than in the coastal mesocosms. The changes over time are exaggerated in the offshore and are nearly perfectly preserved in the coastal, relative to non-normalized measurements. For cell-specific activities, the patterns for the control treatment in the offshore mesocosm now most closely resembles DCEWAF rather than WAF. While the non-normalized activity for WAF showed possibly a slight increase in activity at the later time points, normalization results in a much more significant increase to the point where the activity at hour 96 is the same as at hour 0.

Unlike LAP, BG activities show largely the same patterns over time within treatment between the offshore and coastal mesocosms (Fig. 4). In each treatment, there is a general decrease in activity over the course of the experiment for the coastal and offshore mesocosm respectively: from 42 and 14 to 15 and 1 nM/h in the control treatments, from 70 and 32 to 20 and 2 nM/h in the WAF treatment, from 100 and 80 to 33 and 27 nM/h in CEWAF and from 75 and 32 nM/h to 11 and 22 nM/h in DCEWAF. The primary differences between the offshore and coastal are observed in the CEWAF treatments. CEWAF activity peaks 12 hours earlier in the offshore experiment than in the coastal and, overall, the drop in activity after its peak was more precipitous in the offshore experiment than in the coastal. This difference is seen even more strongly upon cell normalization. While the activities and patterns of the coastal treatments

remain the same when normalized, offshore CEWAF activity becomes even greater relative to the other treatments in the offshore mesocosm. Notably, BG activity peaks in the offshore CEWAF treatment at the same time LAP activity starts decreasing towards its minimum.

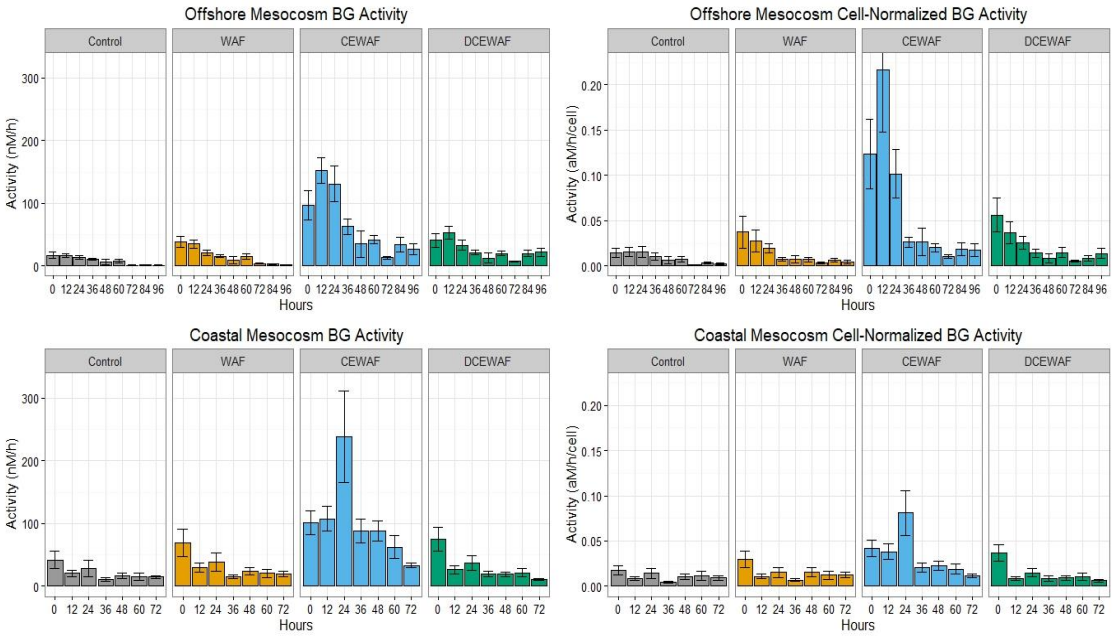

Figure 5. Coastal and offshore mesocosm BG activity timeseries. BG activities measured every 12 hours in offshore and coastal mesocosms. Activities are measured in nM MUF produced per hour while cell-normalized activities are in attaM per hour per cell.

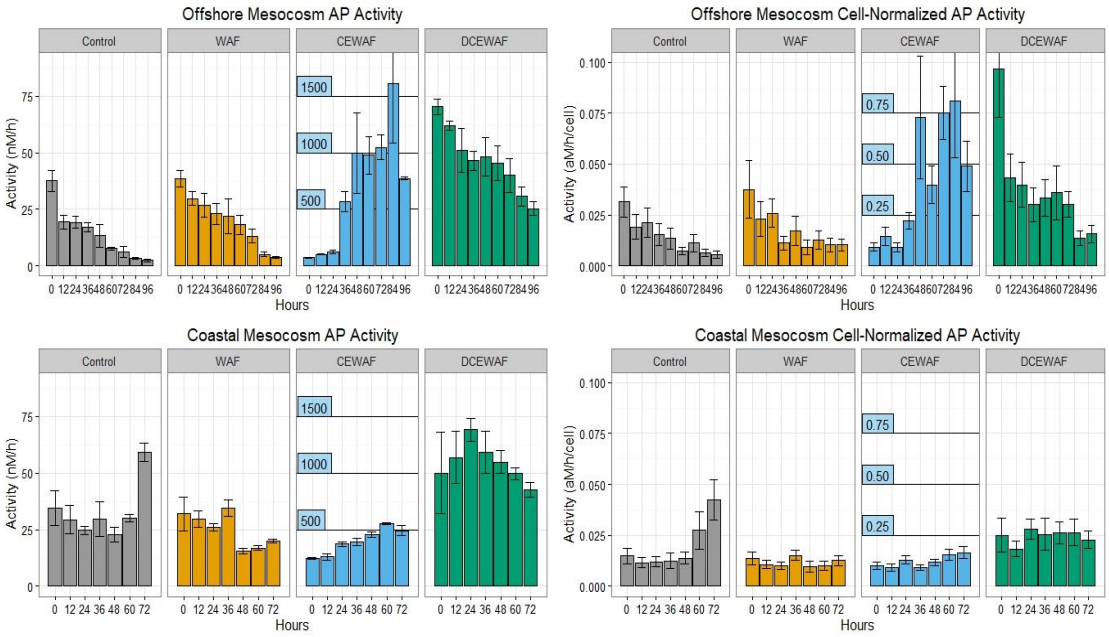

Figure 6. mesocosms. Activities are measured in nM MUF produced per hour while cell-normalized activities are in aM per hour per cell. All CEWAF activities have modified scales due to much higher.

Enzyme activities for AP were variable between experiments and treatments (Fig. 5). In both control and WAF treatments for both experiments, there was a general decrease in activity, although AP activity increases over the last 24 hours in the control coastal treatment. The decrease was greater in the offshore experiment (~40-5 nM/h for control and CEWAF) than the coastal experiment (~30-20 nM/h). CEWAF had the highest activities for all treatments across the mesocosms (AP offshore; 1610 +/- 940, coastal; 555 +/- 45), even when normalized for cell abundance (Fig. 5). Differences in activities between CEWAF and the other treatments were by far the greatest for AP. While activities of CEWAF relative to the other treatments were ~8-fold and ~4-fold greater for BG (Fig. 4) and LAP (Fig. 3) respectively, AP activity in CEWAF was up to 23 (s.e. 13.8) times greater than in the next most active treatment. Like the other two

enzymes, cell-normalization did not substantially change the patterns observed in activity over time. Normalization, however, roughly halved the difference in activity between CEWAF and the other treatments in both mesocosms for AP while it caused no significant decrease in difference for BG or LAP. While total (non-normalized) activities in each treatment have been generally comparable between the two mesocosms, AP activities in offshore CEWAF are up to three times higher than in the coastal counterpart. Patterns of AP over time for the offshore treatments follow a similar pattern to BG, though with a steeper and more consistently linear decrease over time. CEWAF is again the exception, increasing rapidly in the first half of the experiment before flattening off and decreasing. Overall, AP activity in the coastal treatments is shows only small variations through time, with a possible spike in the control treatment at the last time point of 72 hours. Cell-normalization decreases the variation over time, leading to even more constant activities in all but the control, where an increase at the end time points becomes clearer. AP activities in DCEWAF dramatically in the offshore experiment (~70-25 nM/h) while increasing and then decreasing in the coastal experiment.

3.2 Mesocosm kinetics

Differences in each kinetic property were observed between treatments as well as mesocosms. Across the mesocosms, the order of treatments from highest to lowest V_{max} remained constant: CEWAF, DCEWAF, WAF, and Control. This pattern did not hold for K_m, which was highest in the coastal experiment in DCEWAF and in the offshore experiment in CEWAF, but lowest in WAF in the coastal experiment and in DCEWAF in the offshore experiment. These exceptions to the pattern seen in V_{max} for K_m are frequently due to large uncertainties in the estimated K_m values.

Table 2. Enzyme kinetic parameters at initial time point for coastal and offshore mesocosms. In cases where a value is given only for Vmax/Km, the data were too linear for convergence of MM equation. Instances of no measured activity for any substrate concentration are listed as NA. Vmax is in units of nM h-1, Km in µM, and Vmax/Km in nM h-1 µM-1. Standard error is in parentheses below each measurement.

	AP			**BG**			**LAP**		
Coastal	V_{max}/K_m	V_{max}	K_m	V_{max}/K_m	V_{max}	K_m	V_{max}/K_m	V_{max}	K_m
Control	0.444 (0.101)	63.1 (5.5)	142 (30)	4.49 (1.95)	19.2 (2.2)	4.29 (1.80)	6.96 (0.19)	-	-
WAF	0.99 (0.24)	105 (9)	106 (24)	9.31 (1.96)	42.2 (2.4)	4.53 (0.92)	6.87 (0.18)	-	-
CEWAF	8.70 (3.02)	1240 (160)	143 (46)	65.1 (25.2)	547 (64)	8.40 (3.10)	16.1 (0.7)	-	-
DCEWAF	1.72 (0.40)	290 (27)	169 (36)	10.8 (5.9)	103 (17)	9.47 (4.94)	9.71 (0.76)	-	-
Offshore									
Control	3.34 (2.60)	24.7 (2.7)	7.39 (5.70)	50.0 (11.9)	11.2 (0.3)	0.224 (0.053)	4.06 (0.11)	-	-
WAF	4.24 (5.05)	40.7 (8.0)	9.58 (11.3)	60.8 (7.0)	16.8 (0.3)	0.276 (0.032)	5.76 (0.25)	-	-
CEWAF	6.44 (7.04)	97.7 (21.5)	15.2 (16.3)	124 (50)	87.3 (5.3)	0.704 (0.282)	13.2 (0.5)	-	-
DCEWAF	8.81 (6.60)	59.7 (6.23)	6.77 (5.02)	93.0 (23)	30.2 (1.0)	0.325 (0.079)	6.26 (0.31)	-	-

The offshore mesocosm had lower K_m and V_{max} values for most treatments than did the coastal mesocosm. These decreased values were not always proportional however, as the initial slope V_{max}/K_m was higher for the offshore mesocosms than for the coastal mesocosms. When the differences in K_m and V_{max} between mesocosms were proportional, little change was observed in the initial slope. This only occurred in CEWAF and DCEWAF treatments for AP and LAP. Part of the reason for this is difficulty in constraining K_m using nonlinear curve fitting, as seen by the large error on many K_m values (Table 2), which propagates to poorly constrained initial slopes. Despite these uncertainties in initial slope, K_m and V_{max} change substantially for CEWAF and

DCEWAF for AP; V_{max} in CEWAF is 13-fold greater and K_m is nearly 10-fold greater in the coastal treatment relative to the offshore.

3.3 Monoculture and mesocosm activity comparisons

While activities were measured at a single substrate concentration in the mesocosms, activities were measured at five different substrate concentrations in the monocultures, though only the highest measured activities are used for direct comparison with the mesocosms. Additional activity measurements exist for AP from the monoculture repression experiments, where the unrepressed activity could be estimated based on the linear relationship between activity and repressor concentration. Note that control and WAF were the only treatments used in the monoculture experiments, thus all subsequent figures show mesocosm data only for control and WAF.

Because different substrate concentrations were used between the mesocosms and isolates, the activities are the most comparable when corrected for substrate concentration. This can be done for data points with measured kinetic parameters by solving Michaelis-Menten (Eqn. 1) for activity at a given substrate concentration. Activities were normalized to the substrate concentration used to measure activities for the duration of the mesocosm experiments to include as many data points as possible.

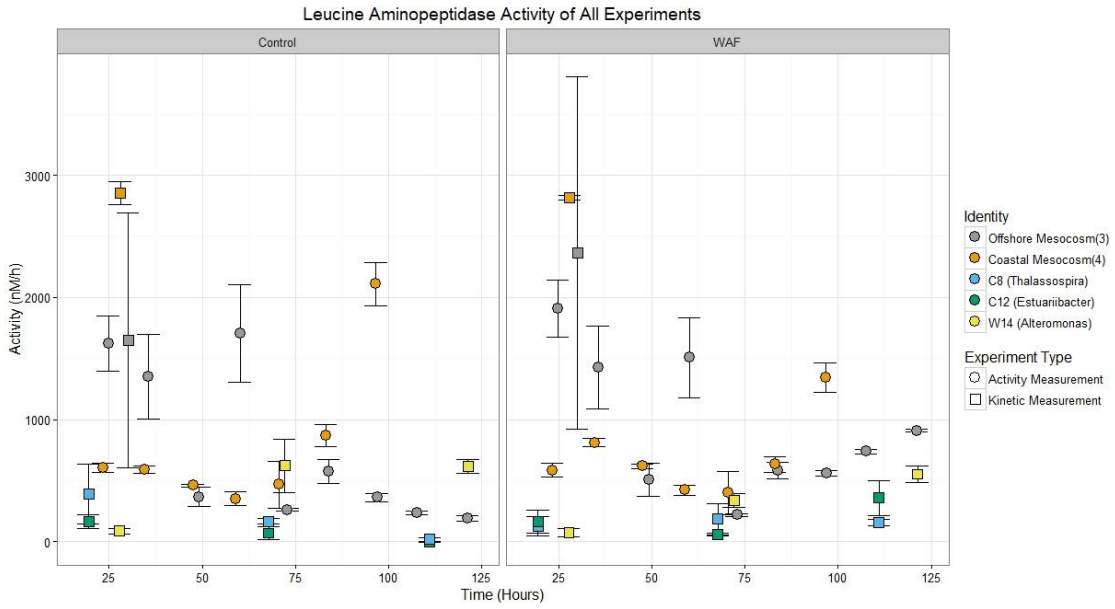

Figure 7. LAP activities over time for all experiments and measurement types. Colors denote bacterial strain or mesocosm experiment, shapes indicate type of measurement.

LAP activities were higher in both mesocosms than any of the monoculture experiments (Fig. 6). As previously noted, the offshore mesocosm decreases in activity over time, while the coastal increases over time (Fig. 3). *Alteromonas* str. W14 is the only strain that definitively increases in LAP activity over time, though it appears to plateau in the control and continue to increase in the WAF. Both *Thalassospira* str. C8 and *Aestuariibacter* str. C12 decrease in activity over time in the control treatment but have constant activity over time in the WAF. Regardless, individual activity measurements of the isolates and coastal mesocosm over time are very similar between control and WAF. The differences between the treatments are subtle and occur mostly in the later time points when activity tends to increase more in WAF than in the control. Substrate concentration normalization to 400µM Leucine-AMC has virtually no effect on any of the LAP activities.

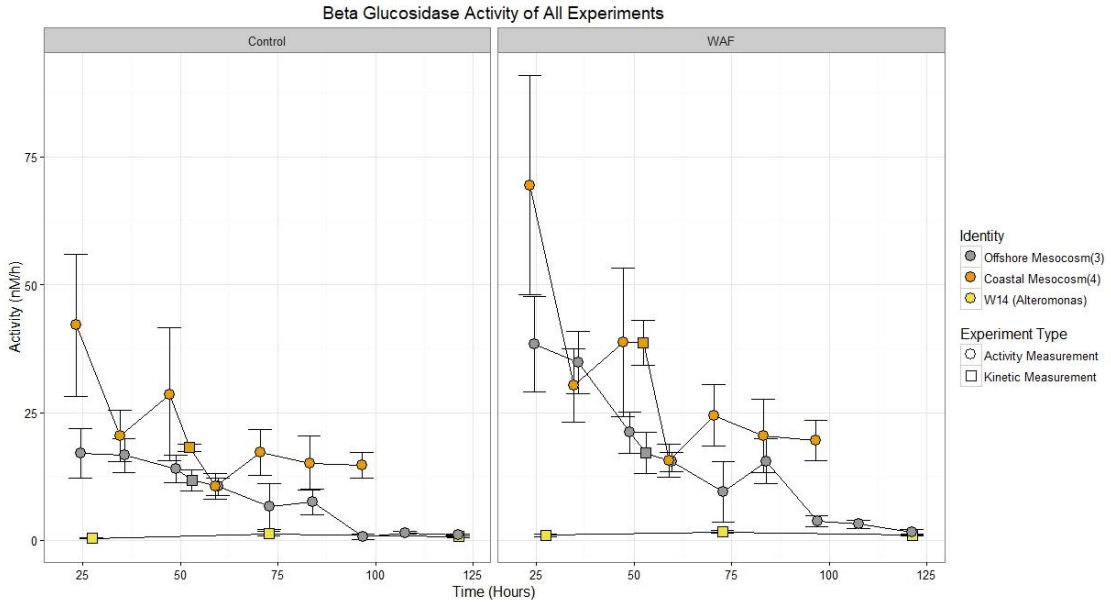

Figure 8. B activities over time for mesocosms and strain Alteromonas str. W14. Preliminary experiments showed no BG activity for Thalassospira str. C8 or Aestuariibacter str. C12 in experimental conditions. Colors denote strain and mesocosm, shapes i

BG activity in the mesocosms were much higher than the monoculture *Alteromonas* str. W14. Both mesocosms decrease in activity over time while *Alteromonas* str. W14 shows consistent and low activity (Fig. 7). Though activity in both mesocosms decreases sharply, the offshore mesocosm decreases to levels on par with *Alteromonas* str. W14. BG measurements for both mesocosms and *Alteromonas* str. W14 were carried out using very similar substrate concentrations at near-saturating conditions, thus normalization for substrate concentration has virtually no effect on any of the activities.

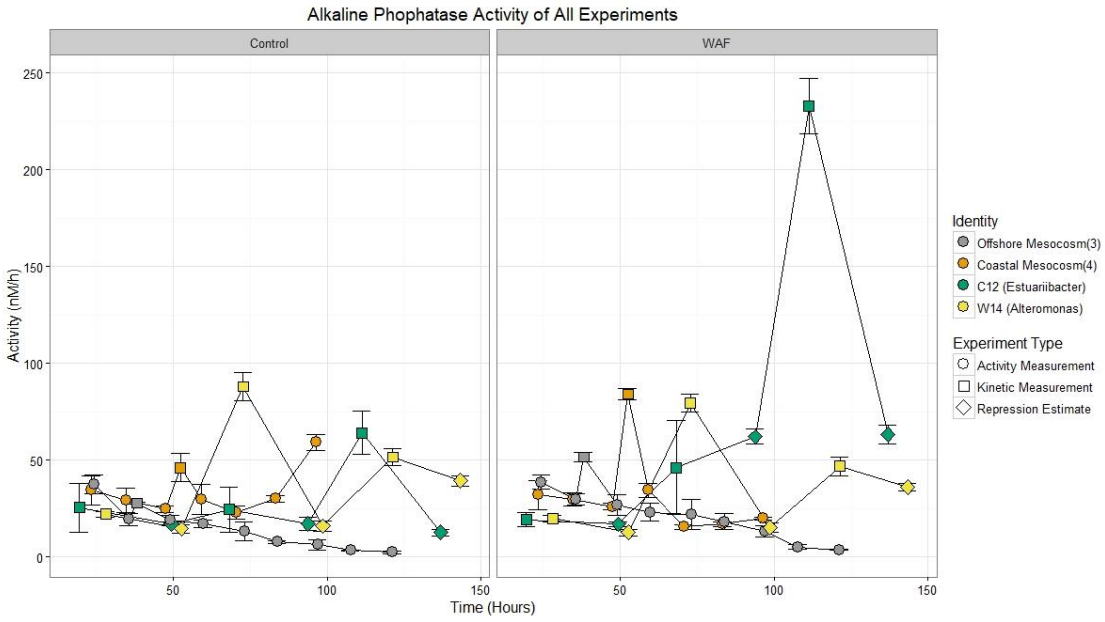

Figure 9. AP activities over time for all experiments and measurement types, except Thalassospira str. C8. Colors denote strain and mesocosm, shapes indicate type of measurement.

Unlike the other enzymes, the AP kinetic measurements (Table 1) for the mesocosms fall within the errors of the activity measurements immediately before and after them in time (see Figs. 6 and 8). Total AP activity in the mesocosms and individual strains were comparable for each treatment. The strains all had greater variability in activity over time than the mesocosms, though this variability is much lower when only one type of measurement is used (e.g. Activity Measurements only, Fig. 6). Patterns over time are very similar for all mesocosms and strains between treatments, though *Aestuariibacter* str. C12 displayed a net increase in activity over time in WAF ($p = 0.00025$) versus a possible, though not significant, net decrease in control ($p = 0.22$).

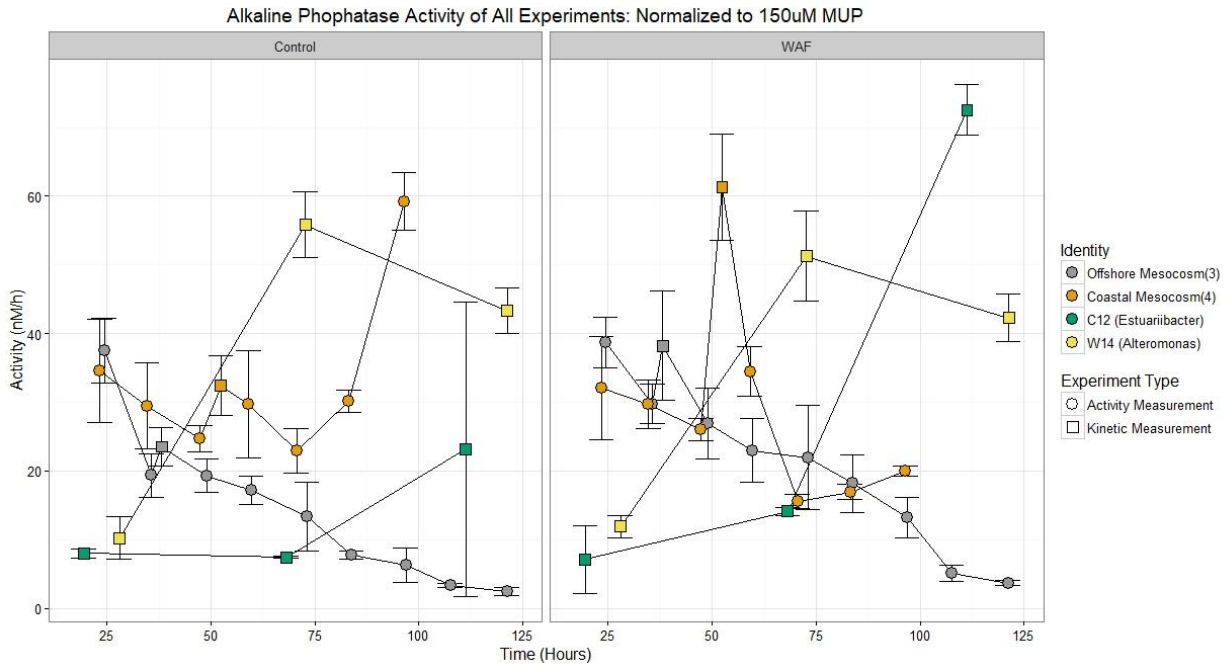

Figure 10. AP activities over time for all experiments, except strain Thalassospira str. C8, normalized using calculated kinetic parameters, Km and Vmax, to calculate activity at 150μM of MUP substrate for comparison across mesocosms, strains, and time points.

Normalizing AP measurements using kinetics calculations changes the patterns between the isolates, mesocosms, treatments, and activity over time the most out of the three enzymes (Fig. 7). This is largely due to the low MUP concentration (150μM) used in the activity measurements in the mesocosms relative to the high MUP concentration (500μM) used to measure activities in the monoculture experiments. As only kinetic measurements are affected, the changes are most evident in the monocultures. In particular, AP activity for *Aestuariibacter* str. C12 changes from a possible decrease over time in the control to constant activity. This is in stark contrast to the WAF treatment, where AP activity by this strain increased over time (in kinetic activity measurements) and upon normalization, this increase was brought down to activities much more comparable with the mesocosms and *Alteromonas* str. W14.

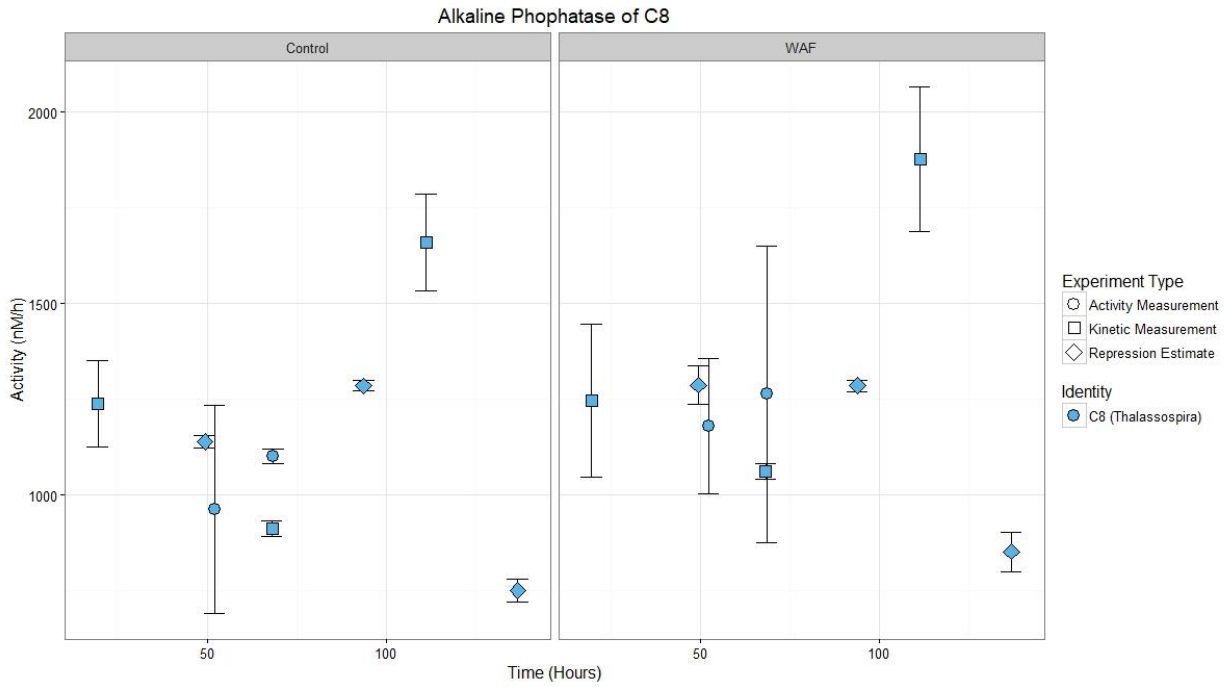

Figure 11. AP activities for Thalassospira str. C8 using all measurement types. The scale is approximately one order of magnitude larger than Figure 4, where the rest of the strains and mesocosms are plotted.

In both control and WAF treatments, AP activity by *Thalassospira* str. C8 is about 10 times greater than any of the other strains or mesocosms; it has the highest raw activity measured in this study with a maximum of 1880nM h^{-1}, one of the highest microbial activities observed in the literature (Alderkamp et al., 2007, Martinez et al., 1996, Meyer-Reil, 1987, Sinsabaugh and Follstad Shah, 2012). Furthermore, discrete V_{max} and K_m values could not be calculated for *Thalassospira* str. C8 AP at any time point because activity was linearly related to substrate concentration for the entire range of concentrations, indicating that substrate concentrations never reached saturation (Table 1). Normalization of substrate concentration decreases *Thalassospira* str. C8 AP activities to one third of their initial values (Fig. 9), decreasing the maximum "observed" activity to approximately one third of the maximum activity observed in

the mesocosms (Fig. 3). While *Thalassospira* str. C8 displays the highest variability in AP activity of all strains and mesocosms, the individual activities are nearly identical between the two treatments. This variability appears to be largely driven by the differences in activity between different measurement types. However, normalization does not reveal a clear pattern in activities over time, even though only the kinetic activity measurements remain.

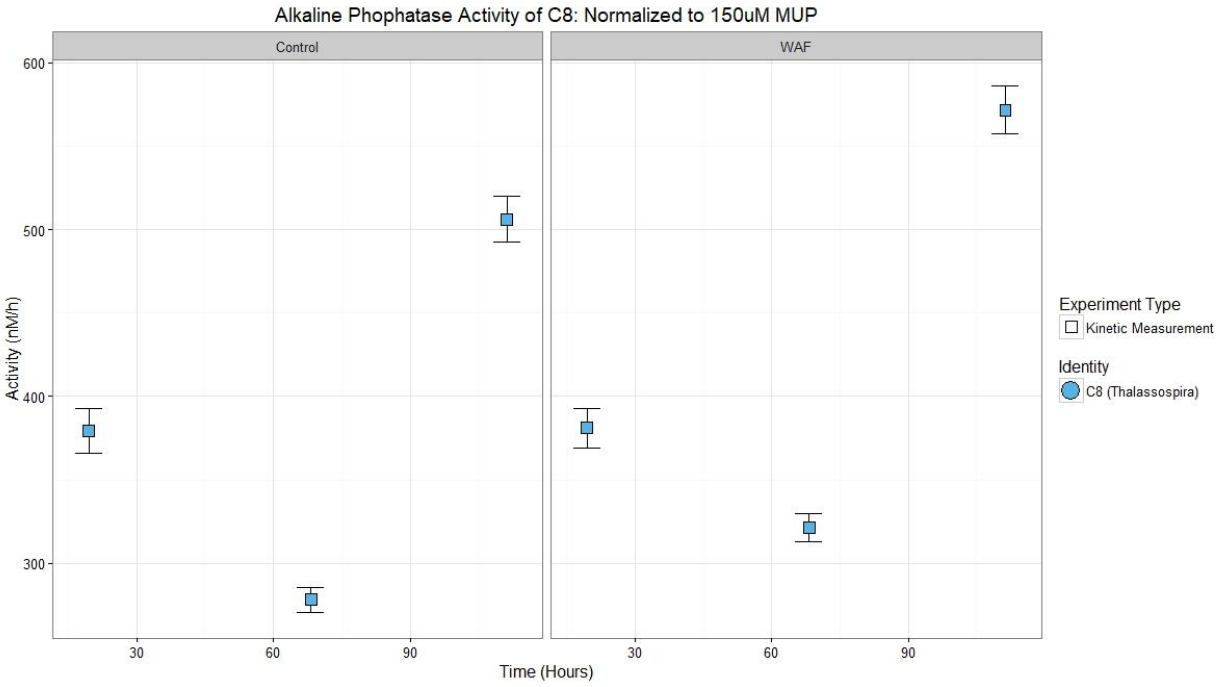

Figure 12. AP activities for Thalassospira str. C8 normalized using calculated kinetic parameters, Km and Vmax, to calculate activity at 150µM of MUP substrate for comparison across mesocosms, strains, and time points.

3.4 Kinetic parameters

Mesocosm kinetics assays were conducted only at one time point early in each experiment, shortly after the t0 time points, while kinetic measurements were made three times throughout the course each monoculture experiment. Cases where the fitting of a two-parameter Michaelis-Menten equation reached convergence are reported with individual V_{max} and K_m estimates, as well as the ratio between the two parameters. *Thalassospira* str. C8 and *Aestuariibacter* str. C12 were challenging to assay as their high activities required rapid turn-around time for individual fluorescence measurements of MUF concentration, and frequently required dilutions up to 40x to be successfully measured on the plate reader. Combined with the fact that substrate concentrations never reached saturating conditions, very few of the kinetic curves for these strains reached convergence for non-linear curve fitting. Even though values are given for offshore control LAP kinetic parameters, curve fitting never reached true convergence as the errors for all parameters are greater than the parameter estimates.

Despite the challenges in calculating individual V_{max} and K_m values for each experiment, every kinetic curve experienced a linear relation of activity to substrate concentration when substrate concentrations were well below K_m. This initial slope parameter, V_{max}/K_m, is an especially powerful point of comparison because it is independent of enzyme concentration (Eqn. 2), a variable that is difficult to estimate under the most controlled cultures and much more so in highly complex systems like the mesocosms. For LAP activity, there are largely few differences in the initial slope between the control and WAF treatments (Table 1), excepting the offshore mesocosm, where both AP and BG have lower slopes and thus lower substrate sensitivity in the control than in WAF.

Table 3 - Enzyme kinetic parameters at initial time point for all mesocosms and monocultures. In cases where a value is given only for V_{max}/K_m, the data were too linear for convergence of MM equation. Instances of no measured activity for any substrate concentration are listed as NA. V_{max} is in units of nM h^{-1}, K_m in µM, and V_{max}/K_m in nM h^{-1} µM^{-1}.

	AP			BG			LAP		
	V_{max}/K_m	V_{max}	K_m	V_{max}/K_m	V_{max}	K_m	V_{max}/K_m	V_{max}	K_m
Coastal Control	0.44 (0.10)	63.1 (5.5)	142 (30)	4.49 (1.95)	19.2 (2.2)	4.29 (1.80)	9.47 (3.64)	11,500 (2700)	1220 (370)
Coastal WAF	0.99 (0.24)	105 (9)	106 (24)	9.31 (1.96)	42.2 (2.4)	4.53 (0.92)	9.36 (3.07)	11,300 (2300)	1210 (310)
Offshore Control	3.34 (2.60)	24.7 (2.7)	7.39 (5.70)	50.0 (11.9)	11.2 (0.3)	0.224 (0.053)	4.27 (7.44)	40,600 (49,000)	9500 (12000)
Offshore WAF	4.24 (5.05)	40.7 (8.0)	9.58 (11.3)	60.8 (7.0)	16.8 (0.3)	0.276 (0.032)	8.77 (1.51)	7230 (717)	824 (116)
Thalassospira str. C8 Control	2.53 (0.09)	-	-	NA	NA	NA	-	-	-
Thalassospira str. C8 WAF	2.54 (0.08)	-	-	NA	NA	NA	0.594 (0.110)	71.4 (4.2)	120 (21)
Aestuariibacter str. C12 Control	0.053 (0.004)	-	-	NA	NA	NA	-	-	-
Aestuariibacter str. C12 WAF	0.049 (0.032)	29.8 (12.1)	479 (352)	NA	NA	NA	0.237 (0.045)	-	-
Alteromonas str. W14 Control	0.091 (0.033)	43.9 (7.8)	494 (157)	0.020 (0.020)	0.586 (0.180)	30.7 (22.1)	0.329 (0.105)	-	-
Alteromonas str. W14 WAF	0.141 (0.029)	27.8 (2.3)	200 (39)	0.033 (0.015)	1.48 (0.16)	48.2 (14.3)	0.443 (0.041)	-	-

All the strains have much lower initial slopes for BG and LAP than any of the mesocosms. Conversely AP initial slopes vary enough within the mesocosms and strains such that their ranges overlap and *Thalassospira* str. C8 clusters with the greater slopes in the

mesocosms rather than the lower slopes of the strains. These low slopes in the strains *Aestuariibacter* str. C12 and *Alteromonas* str. W14 are driven by extremely high K_m values as their V_{max} values are comparable to those of the mesocosms and *Thalassospira* str. C8. Whatever kinetic differences may exist between control and WAF are most visible in K_m and V_{max} values. While these parameters tend to scale between control and WAF resulting in statistically indistinguishable initial slopes, WAF frequently has the significantly higher V_{max}. The exception is *Alteromonas* str. W14 in AP where the control has a higher V_{max} than WAF, although interestingly it is higher by nearly the exact same fraction, 0.6, that WAF is over control for AP in both coastal and offshore mesocosms. The BG kinetic parameters in the coastal mesocosm show the clearest differences between WAF and control. The initial slope is about twice as high in the WAF as in the control, even though, unlike any other sample, its K_m values are the same. The differences in substrate sensitivity are visible only when initial slope is used as a proxy, rather than K_m alone as is often done in the literature (Martinez and Azam, 1993, Ammerman and Glover, 2000).

Despite changing absolute LAP activities (Fig. 4), sensitivity to substrate concentration remains mostly constant over time, with a slight decrease in *Thalassospira* str. C8 in the control (Fig.10). The exception to this rule is *Alteromonas* str. W14 which has as a V_{max}/K_m of about 0.5 at time point 1, which then jumps by nearly 10-fold by day 3 and then remains constant. While the data are incomplete, there are no significant differences between the control and WAF for any treatment (range of $p = 0.17 – 0.98$). The variability in LAP sensitivity appears most closely tied to the absolute activity of each experiment. The two mesocosms have much higher LAP activities at the first time point than the strains, and they have correspondingly high V_{max}/K_m. At

the first time point all three strains have similar LAP activities, and then *Alteromonas* str. W14 increases by about 8-fold by the third day and remains constant while *Thalassospira* str. C8 and *Aestuariibacter* str. C12 activities remain low and constant (Fig. 5.), in exactly the same pattern seen in V_{max}/K_m.

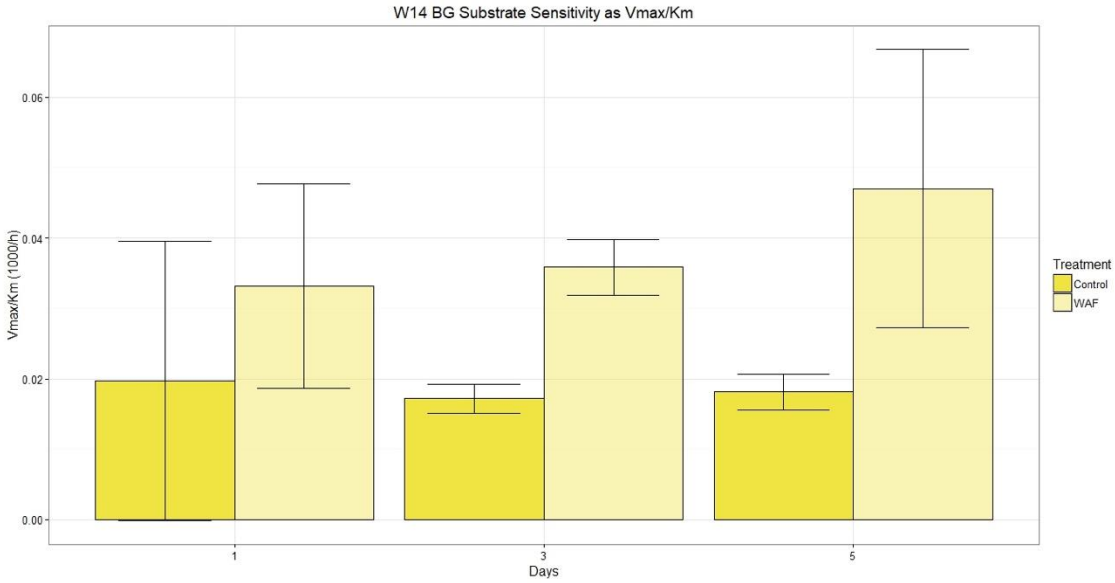

Figure 13. Alteromonas str. W14 BG sensitivity over time as Vmax/Km. Compare to initial values for coastal mesocosm of 4.5 and 9.3 for offshore.

Unlike LAP, AP substrate sensitivity changes considerably over time for each strain. Additionally, AP V_{max}/K_m is not as tightly tied to absolute activity as was LAP (Figs. 5 and 7). *Thalassospira* str. C8 has exponentially higher AP activity than all the other experiment at all times, yet it is only approximately two times greater than *Alteromonas* str. W14 in AP sensitivity on days 3 and 5 (Fig. 12). *Aestuariibacter* str. C12 sensitivity remains very low, though it increases over time, especially on day 5 in WAF. This may be internally proportional to the large increase in absolute AP activity in *Aestuariibacter* str. C12 WAF on day 5, but *Aestuariibacter* str. C12 still has the lowest V_{max}/K_m despite having the highest absolute activity after

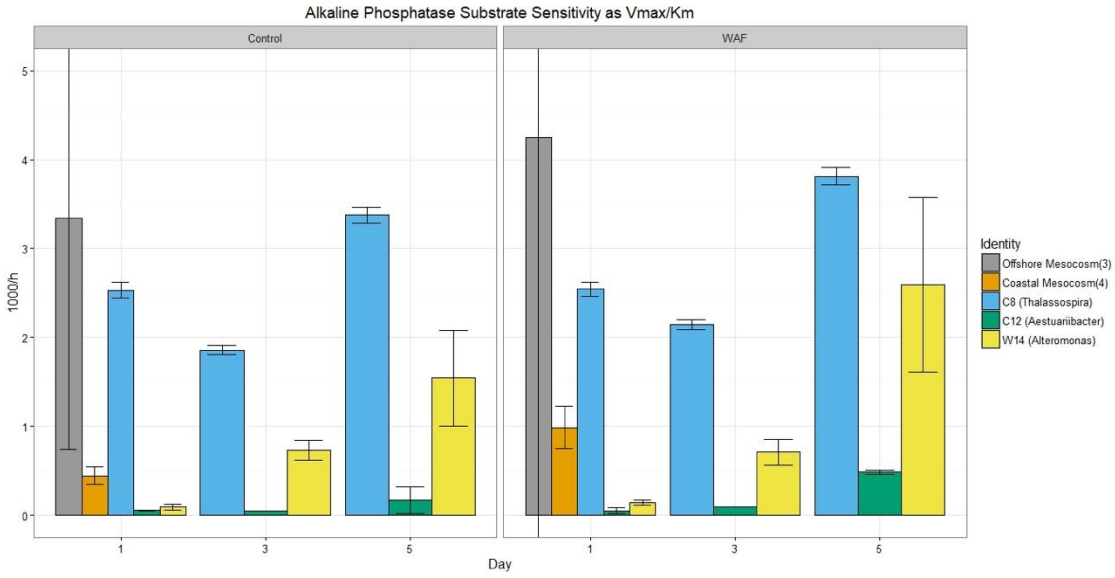

Figure 14. AP substrate sensitivity over time as Vmax/Km for all experiments. Large error bars particularly on the offshore mesocosm are due to the difficulty of constraining Km.

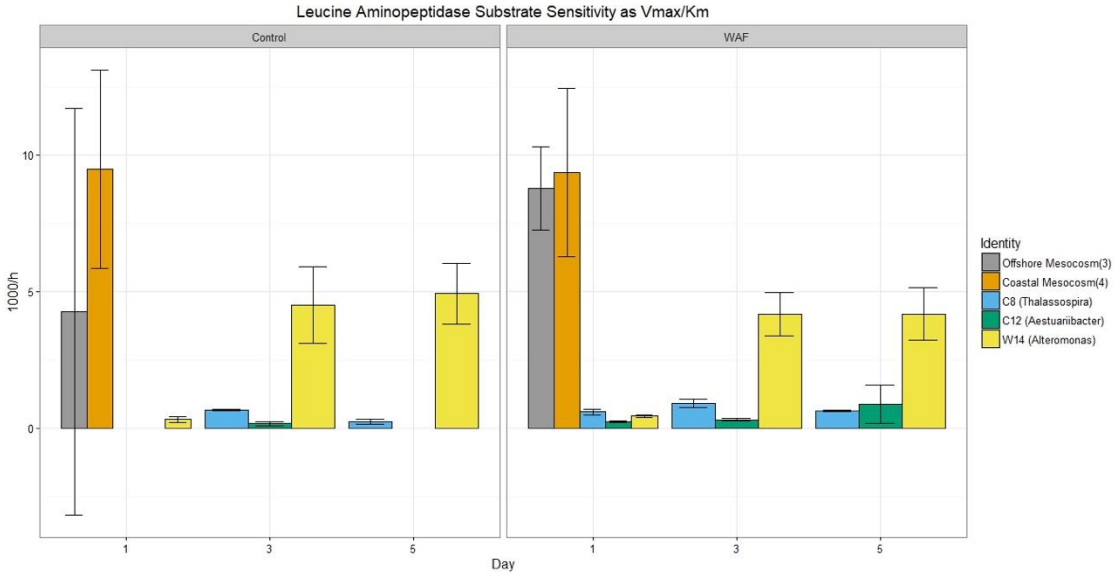

Figure 15. LAP substrate sensitivity over time as Vmax/Km for all experiments. Large error bars are due to the difficulty of constraining Km. Missing bars for strains indicate that errors on all kinetic.

Thalassospira str. C8. This sort of internal proportionality between absolute activity and estimated sensitivity also appears in *Thalassospira* str. C8, where the pattern in sensitivity exactly mirrors that of absolute activity (Figs. 8 and 12). Proportionality does not hold for *Alteromonas* str. W14, which has absolute activity that peaks at day 3 before decreasing to day 1 levels (Fig. 6), whereas its sensitivity increases linearly.

Alteromonas str. W14 shows little to no significant differences in enzyme sensitivity between the control and WAF treatments for AP or LAP, though over time BG V_{max}/K_m increases to about double that of the control (Fig. 11). Although the changes in WAF over time aren't statistically significant, the sensitivity appears to slightly increase linearly. *Alteromonas* str. W14 sensitivity at the t=1 day is about 0.02, while the mesocosms are more than 2000-fold higher, even though BG activity at that time is only about 20 times higher in the mesocosms than in *Alteromonas* str. W14 (Figs. 5 and 11).

3.5 Estimated unrepressed activity

Unrepressed activities were estimated for each strain, treatment, and repressor at each time point to quantify the change in activity in the presence of the repressor. When a simple linear model was fit to the activities at each concentration of repressor, the y-intercept defines the repressed activity at zero substrate concentration (Fig. 13). Even though all strains experienced decreased AP activity in the presence of phosphate and few in the presence of glucose, this linear model yielded similar estimates of unrepressed activity for *Thalassospira* str. C8 and *Aestuariibacter* str. C12 (Figure 14 A&B). *Alteromonas* str. W14 showed consistently lower estimates of unrepressed activity when calculated using phosphate versus glucose data (Figure 14C). This appears to be due to the non-linear response of AP activity to increasing

concentrations of phosphate. Figure 13 shows that greatest response in terms of AP repression occurs at low phosphate concentrations, and between 1000 and 10,000uM phosphate, there is relatively little further repression. Fitting a linear equation to this data will therefore chronically

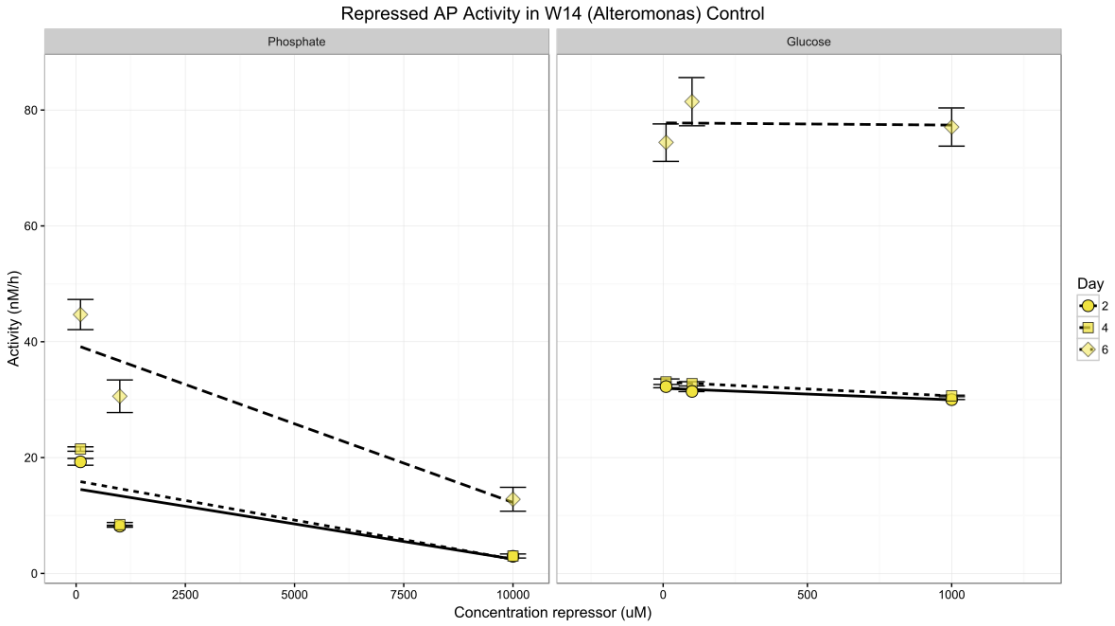

Figure 16. Example of estimating unrepressed activity from repression data in Alteromonas str. W14. Linear equations were fit for each time point and used to calculate activity when the concentration of repressor is zero, i.e. the y-intercept. Note that different

underestimate the unrepressed activity. This is exactly what is seen when comparing the values calculated with the phosphate repression data versus the glucose repression data (Figure 14C). Therefore, activity repression has been normalized as the decrease in activity relative to the unrepressed activity, as calculated using the glucose repression data (Fig. 15). *Thalassospira* str. C8 had the lowest relative repression by phosphate; just ~40% repression compared to the 80-90% reached by *Aestuariibacter* str. C12 and *Alteromonas* str. W14. *Thalassospira* str. C8 and *Alteromonas* str. W14 had mostly constant rates of relative repression over time in both the

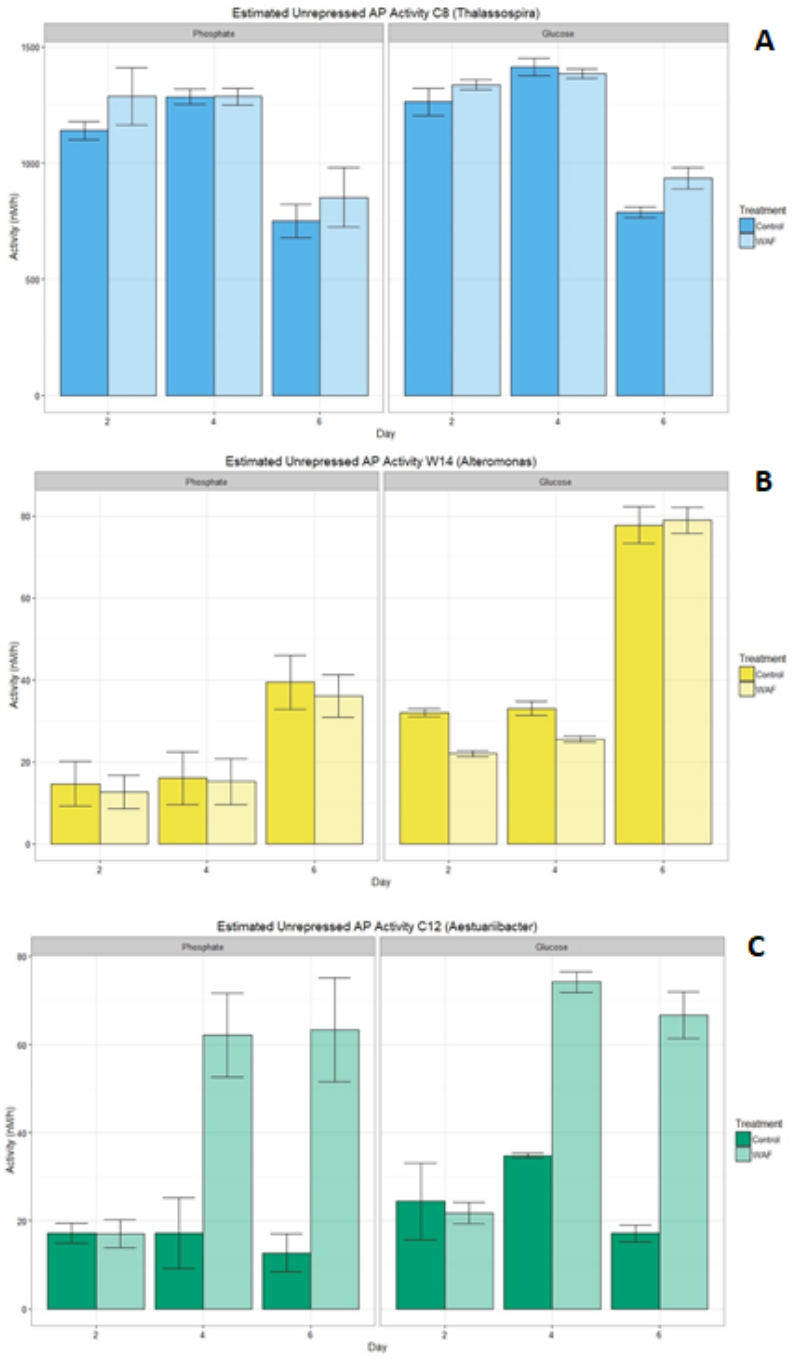

Figure 17. Estimated unrepressed AP activity in each strain. Panels are divided by estimates using the linear equation from the phosphate repression curve and from the glucose curve.

control and WAF. *Aestuariibacte*r str. C12 was the only strain to show significant variation between control and WAF in relative repression by either phosphate or glucose. Relative repression by phosphate in *Aestuariibacter* str. C12 decreased over time in both control and WAF, though the control had a maximum in repression at day 4 whereas relative repression decreased linearly in WAF. Neither *Thalassospira* str. C8 nor *Alteromonas* str. W14 experienced any significant change in AP activity in the presence of glucose. *Aestuariibacter* str. C12 appeared to experience low levels of relative repression at day 2, ~25%, though this repression disappeared by the next time point in the control. In *Aestuariibacter* str. C12 WAF, the low-level repression by glucose at day two decreased over time until statistically significant "negative repression" of ~25% was observed at the final time point (Fig. 15). "Negative repression" is simply an operational term that defines enhancement of activity. Thus, over the three time points, *Aestuariibacter* str. C12 in WAF experiences repression by glucose, followed by increasing enhancement of activity by the same concentration of glucose.

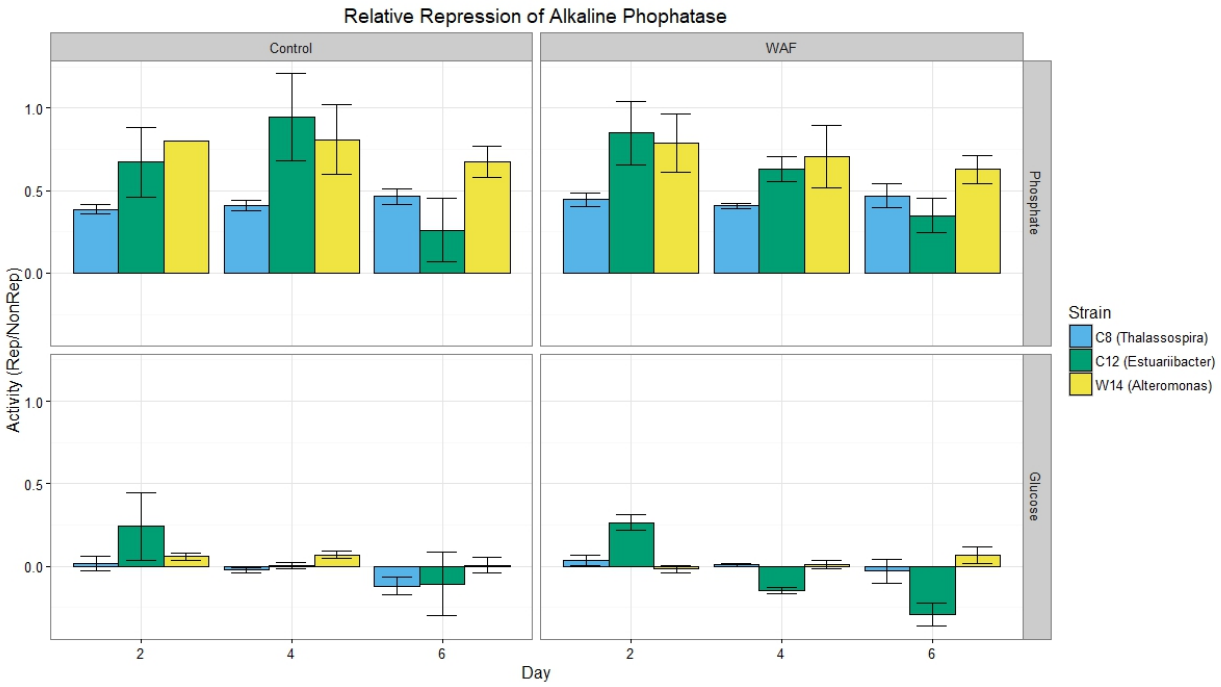

Figure 18. Relative repression of AP activity by glucose and phosphate in each monoculture and treatment at the three repression time points. Repression is expressed as the difference between activities with zero repressor and with the highest concentration of repressor, relative to the unrepressed activity. Thus a value of 1 is complete repression i.e. zero activity and a value of 0 is no repression, i.e. repressed activity=unrepressed activity. Values <0 indicate "negative repression", which is when activity increased in the presence of the repressor rather than decreased.

4. DISCUSSION

4.1 Mesocosm summary

The mesocosms employed here are highly complex systems composed of diverse microbial communities designed to mimic surface ocean conditions during an oil spill. These short term, intensively sampled experiments were designed to gain insight into the initial stages of oil degradation, when the chemical conditions are changing the most rapidly. Until recently, analysis of community shifts and activity following exposure to oil did not sample within this initial timeframe (Wang et al., 2016, Boopathy et al., 2012, Edwards et al., 2011, Kleindienst et al., 2015). However, Doyle et al., (2018) showed that responses in community composition and enzyme activity occur within hours after exposure. As tools for the measurement of the rates of basic metabolic processes, exoenzymes are excellent indicators of the microbial community's basal energy and nutrient demands during the initial steps of oil degradation. The enzymes BG, LAP and AP each account for a major element in microbial growth and homeostasis: carbon and energy for BG, nitrogen for LAP, and phosphate for AP. Thus changes in activity for each enzyme over time indicate changing demands for C, N, and P.

4.2 Mesocosm overall exoenzyme activities

Measured activities of each enzyme show rapid and dynamic responses to conditions in the mesocosms, both in changes over time and in differences in kinetic properties between the treatments. While changes in activities over the course of the incubation did not differ very much between control and WAF treatments (Figs. 3-5), it is nevertheless likely that oil has some effect on the absolute exoenzyme activities, even if the conditions of this experiment do not result in

enough resolution to observe it. Initial oil amounts, measured as estimated oil equivalents (Wade et al., 2011), were ~10X higher in DCEWAF than WAF and 5-10X higher in CEWAF than DCEWAF (Table 5). For reference, EOE was 0.1-10 mg/L for most samples above detection within the subsurface plume during the DWH event (Wade et al., 2016). The extra oil and Corexit in the DCEWAF and CEWAF treatments is associated with far higher activities than the other treatments, particularly of AP (Fig. 3). However few differences are seen in the either the level of activity or activity trends over time between the Control, WAF, and DCEWAF treatments. Even though DCEWAF contains >10x the oil of the WAF treatment, the absolute difference in oil amount is only about 5-8 mg/L compared to the full ~30-75 mg/L difference between DCEWAF and CEWAF (Table 3). This relatively small difference in oil between WAF and DCEWAF thus reflects the relatively small differences in the enzyme results between the two treatments.

Table 4. Initial mesocosm oil concentrations as estimated oil equivalents (EOE) in units of mg/L

Mesocosm	Treatment	Initial oil (mg/L)
Offshore	WAF	0.739
	CEWAF	39.07
	DCEWAF	6.17
Coastal	WAF	0.29
	CEWAF	81.06
	DCEWAF	8.13

While these results cannot speak to the specific mechanisms of this increase, our experiments reveal that exposure to high concentrations of oil and dispersant significantly changes both the pattern and magnitude of microbial metabolic demands over the early stages of oil degradation. It is then likely that exposure to oil, above some base concentration that is

community-dependent, results in community net changes in metabolic activities relative to carbohydrates, organic N, and P. Moreover, the changes observed in this study cannot be accounted for by prokaryotic cell concentrations alone, as cell-normalization does not resolve the far greater activities of CEWAF relative to the other treatments (Figs. 3-5). Other studies have found cell normalization to significantly impact the interpretation of exoenzyme activity, such as increasing carbon demand in the deep ocean (Baltar et al., 2009), but the low impact of cell normalization on patterns of exoenzyme activity observed here indicate that the purpose of the exoenzyme usage (e.g. AP used to meet P quotas instead of C quotas) did not vary significantly during the course of our experiments. This is may be because environmental microbial communities are too complex in structure and dynamic over time for absolute cell concentration to be consistently related to enzyme concentration, or it may be because the mesocosms have high organic C levels, thereby eliminating the need for LAP or AP to be used for C acquisition, or it could be some other reason not assessable with our dataset. However, the insensitivity of enzyme activity to cell abundance is direct evidence that fractions of the microbial community are changing their expression of exoenzymes over the course of the mesocosms - if expression/activities were invariant, then they should follow cell counts directly. Studies of microbial metabolism in the surface waters near the blowout site also observed insensitivity of AP activity to cell abundance and microbial biomass (Edwards et al., 2011) as evidence of P-limited growth. Microbial growth on the Louisiana-Texas Shelf affected by the DWH blowout is known to be limited by bioavailable phosphorus and nitrogen concentrations (Sylvan et al., 2006). The addition of massive amounts of carbon in the form of crude oil to such a system exacerbates the nutrient-limitation of the microbial community, resulting in low growth

efficiency as the excess C is respired away without a corresponding increase in microbial biomass (Del Giorgio and Cole, 1998, Edwards et al., 2011).

4.3 Mesocosm source community signatures

Few overall differences in enzyme activities over time by treatment were observed between the two mesocosms, where the offshore and coastal source water represented microbial communities from a low-nutrient and high-nutrient environment respectively. However, differences were apparent in the estimated kinetic parameters (Table 2). A distinct signature of source conditions persists, even after approximately a day of growth in the mesocosms and the likely changes that occurred during the setup of each mesocosm (Doyle et al., 2018). The low nutrient communities in the offshore experiment maintained kinetics favorable to low nutrient environments, despite growing in the same conditions as the high nutrient communities (amended nutrients, oil with or without Corexit). Not only are the V_{max} and K_m values lower in the offshore mesocosms, these values do not scale as the initial slope, V_{max}/K_m, is greater than the coastal mesocosms. The relatively lower K_m, which results in enhanced substrate sensitivity, is an adaptive trait for low nutrient environments (Chróst and Rai, 1993, Marx et al., 2005, Sebastián et al., 2004b). This source community signature is the greatest in the non-dispersant amended treatments, Control and WAF. While relative differences in K_m and V_{max} are the greatest for CEWAF, particularly for AP (Table 2), these differences tend to be proportional compared to the other treatments, resulting in little differences in sensitivity. Conversely, K_m and V_{max} for the Control and WAF treatments are proportionally distinctly different between the offshore and coastal experiments, resulting in the greatest differences in sensitivity between the two mesocosms. This sensitivity is perhaps the best measure of functional differences between

Table 5. Comparative literature exoenzyme activity data

AP Activity Range (nM/h)	BG Activity Range (nM/h)	LAP Activity Range (nM/h)	LAP:BG	Location	Source
2.43 – 38.7	0.793 – 38.4	189 – 1910	22.8 – 557	Offshore GoM Mesocosm	This Study
15.6 – 59.3	10.6 – 69.4	352 - 2110	8.44 - 143	Coastal GoM Mesocosm	This Study
200 - 1000		30 - 400		Louisiana Shelf	(Ammerman and Glover, 2000)
220 – 450				Lake Travis, TX	(Ammerman and Glover, 2000)
	63.3	17.5	213	ALOHA	(Christian and Karl, 1995)
	0.03	6.7	0.276	Equatorial Pacific	(Christian and Karl, 1995)
	0.005– 0.049	1.5 - 27	434 - 1052	Antarctica	(Christian and Karl, 1995)
7.14 – 428.4				Mesotrophic Lake	(Chróst and Overbeck, 1987)
		0.15		Brackish Baltic Fjord	(Hoppe et al., 1988)
	0.26	300	1150	GoM DWH Deep Plume	(Ziervogel and Arnosti, 2016)
	0.17	67	386	GoM DWH Deep Non-Plume	(Ziervogel and Arnosti, 2016)
	1.71e-4 – 0.0104	0.00156 – 0.144		Deep GoM Mesocosm Control	(Kleindienst et al., 2015)
	0.00428 – 0.0834	5.96e-4 - 3.88		Deep GoM Mesocosm WAF	(Kleindienst et al., 2015)

the measured enzymes in each treatment because V_{max} and K_m alone are subject to confounding variables such as population size, enzyme concentration, and non-conformity to Michaelis-Menten kinetics (Christian and Karl, 1995). The initial slope of the kinetic curve is independent of all these factors, making it the most powerful point of comparison between kinetic measurements (Sebastián et al., 2004b). Thus, enzyme activities in the Control and WAF treatments show the greatest preservation of source community kinetics for each enzyme, whereas the enzyme kinetic profile of CEWAF and DCEWAF changed during the course of each experiment.

Both mesocosms fell within the reported range for AP activity in environmental samples, though they were at the low end of the range for surface ocean environments (Table 5). Remarkably, both mesocosms had maximum LAP activities up to 5 times greater than any previous report for environmental samples. The low end of LAP activity range for both offshore and coastal mesocosms was similar to the highest measurements from the surface Gulf of Mexico pre-oil spill, as well as measurements from the deep plume during the 2010 Deepwater Horizon blowout.

4.4 Monoculture repression

AP activity in each strain was repressed by phosphate to a different extent. *Thalassospira* str. C8 experienced the least relative repression, with only a ~45% decrease in activity on average. This may be an artifact of its extreme absolute AP activities as it is possible that the concentrations of phosphate used were insufficient to swamp out the number of AP enzymes present. This is striking as such high concentrations of phosphate were used because preliminary experiments showed extremely high AP activities in *Thalassospira* str. C8 and *Aestuariibacter*

str. C12. Moreover 10mM phosphate begins to experience solubility constraints, as visually and anecdotally demonstrated when the 200μL aliquots of the 10mM phosphate samples in the 96-well plates turned bright white with phosphate precipitates upon the pH increase caused by borate buffer addition. Another explanation is that AP is not fully repressible with phosphate in *Thalassospira* str. C8 under experimental conditions. This implies a secondary function for the production of AP, although catabolite acquisition seems unlikely as the addition of the readily metabolizable glucose did not affect AP activity (Fig. 12).

The only added carbon source for the media used in the monoculture experiments was oil, but the seawater used is coastally sourced and has appreciable amounts of dissolved organic carbon. Moreover, as all three strains are oil-degraders, the cultures were not hypothesized to be limited in catabolites in the WAF treatment. Glucose was tested as a repressor of AP because one or more of the isolates could potentially be very limited in its suite of degradable hydrocarbons and therefore could run out of C if all of the degradable components were exhausted, or because the increased P supply generated by AP activity may alter C:N:P stoichiometry, making C limiting. AP activity in *Thalassospira* str. C8 and *Alteromonas* str. W14 did not respond to presence of glucose, but it did in *Aestuariibacter* str. C12. At the first repression time-point, two days after inoculating the cultures, AP activity in *Aestuariibacter* str. C12 decreased modestly by about 20% upon addition of glucose in both control and WAF. Two days later, its AP activity in the control appeared unaffected by glucose, similar to *Thalassospira* str. C8 and *Alteromonas* str. W14. At the same time point, however, AP activity in WAF significantly increased in the presence of glucose by about 15%. At the end of the experiment, AP activity of *Aestuariibacter* str. C12 in WAF with added glucose had increased nearly 35% over the unrepressed activity.

While this was happening, *Aestuariibacter* str. C12 AP in WAF was becoming less repressible by phosphate at nearly the same rate as with glucose. This may be catabolite or energy limitation, though it seems unlikely that AP is being used for catabolite acquisition. If growth of *Aestuariibacter* str. C12 in WAF becomes limited by easily metabolized organic carbon, the addition of glucose could spur a rapid response in cell activity and growth. The wait time between glucose addition and activity measurement is likely sufficient for such a response given the reasonable growth rates of the strain. Increasing metabolic activity increases the demand for nutrients, which can explain the increase in AP activity as a mechanism for correcting the C:P imbalance caused by the addition of pure C in the form of glucose. Additionally absolute AP activities increase at the later time points in *Aestuariibacter* str. C12 (Fig. 7), indicating an overall increasing P-demand. This could be tied to the decreasing repressibility of *Aestuariibacter* str. C12 AP with phosphate in a similar manner that *Thalassospira* str. C8 was only minimally repressible and had extremely high absolute activities. The mesocosms enzyme experiments were designed primarily to examine community activity of AP, BG, and LAP over time. Kinetics experiments were conducted to assess enzyme sensitivity on top of temporal changes.

Conversely the monocultures were designed to give the mesocosm activities context by measuring the enzymatic potential of oil-degrading strains in terms of changing kinetic properties and repressibility over time. Thus the two experiments complement each other, but the strengths of each are the weaknesses of the other. In particular, the mesocosms have 12-hr resolution of the activities of each enzyme at a constant specific concentration, while the

monocultures only have the individual activities of different substrate concentrations at 48-hr resolution.

To better apply the kinetic and repression data from the monoculture experiments to a comparison of activity with the mesocosms, it important to maximize the number of activity time points in the monocultures. For BG and LAP, kinetic measurements, only, were available. Therefore, the activity at the highest substrate concentration was defined as the activity for that time point. AP activity was measured every 24 hours, with at least one measurement at each time point using the same substrate concentration, although half of them are derived from the repression experiments. The resolution of AP activity over time could be increased to 24-hr if an unrepressed activity could be estimated for each repression time point. AP was repressed with both phosphate and glucose, which affected the activity to different degrees. These two repression experiments were carried out simultaneously at each time point so it is reasonable to assume that each should have the same unrepressed activity. As a first estimate, activity over repressor concentration was fit with a simple linear equation where by definition the y-intercept represents the unrepressed activity.

Figure 11 A-B shows reasonably consistent estimates of unrepressed activity when using the linear fit from either the phosphate or glucose data. However, the simple linear approach is not appropriate for *Alteromonas* str. W14 as the linear model for phosphate consistently underestimates the unrepressed activity relative to the linear model for glucose. *Alteromonas* str. W14 showed the greatest repression of AP at the lowest concentration of phosphate of the three strains. It is likely then that the linear decrease in activity occurs at lower phosphate concentrations than 100μM, the lowest concentration used in this experiment. Therefore, if

repression curves are to be used for estimating unrepressed activity, the estimates must be confirmed using multiple independent repressors, especially if either of them are predicted to be strong repressors. While it then follows that underestimating unrepressed activity would result in overestimating relative repression, it turns out that the activities of *Alteromonas* str. W14 and *Aestuariibacter* str. C12 at the highest concentration of phosphate are so low that relative repression still comes out to ~90% even using the significantly higher glucose estimate of unrepressed activity.

5. CONCLUSION

The mesocosms were highly complex systems of diverse microbial communities changing with oil degradation, aggregate production, and variable redox conditions. The three core metabolic exoenzymes, AP, BG, and LAP reflected this complex system in their highly variable activities between treatments and over time, as well as in their distinctive kinetic parameters. As an effort to detangle the conceptually confusing community activities and kinetics, three oil-degrading isolates from a mesocosm were analyzed for their enzyme dynamics. While these strains did not approach the mesocosms in terms of heterotrophic activity via BG or LAP, the similar AP activities indicated that P demand and acquisition is an important anchor point for comparisons between the two experiments. This is supported in the AP kinetic parameters, where the strains showed as much variability on the same scales as the mesocosms in sensitivity to substrate concentrations. While individual strains varied little in their BG and LAP kinetic parameters over time, the diversity between the three strains scaled up is on the same order as the different mesocosm treatments. These three strains have demonstrated enzymatic potential of AP in terms of flexibility in kinetic parameter and absolute activity to significantly contribute to observed AP dynamics in the mesocosms. The concurrent lack of dynamic BG and LAP activity, however, suggests either that these oil-degraders have different energy acquisition strategies than the mesocosms even under control conditions, or that the culture conditions did not provide adequate substrates for the strains to display their heterotrophic enzyme potential.

REFERENCES

ALBERTSON, N. H., NYSTRÖM, T. & KJELLEBERG, S. 1990. Exoprotease activity of two marine bacteria during starvation. *Applied and Environmental Microbiology,* 56**,** 218-223.

ALDERKAMP, A.-C., VAN RIJSSEL, M. & BOLHUIS, H. 2007. Characterization of marine bacteria and the activity of their enzyme systems involved in degradation of the algal storage glucan laminarin. *FEMS Microbiology Ecology,* 59**,** 108-117.

ALLISON, S. D. 2005. Cheaters, diffusion and nutrients constrain decomposition by microbial enzymes in spatially structured environments. *Ecology Letters,* 8**,** 626-635.

AMMERMAN, J. W. & GLOVER, W. B. 2000. Continuous underway measurement of microbial ectoenzyme activities in aquatic ecosystems. *Marine Ecology Progress Series,* 201**,** 1-12.

AMON, R. M. & BENNER, R. 1994. Rapid cycling of high-molecular-weight dissolved organic matter in the ocean. *Nature,* 369**,** 549.

ARNOSTI, C. 2011. Microbial extracellular enzymes and the marine carbon cycle. *Annual Review of Marine Science,* 3**,** 401-425.

ARNOSTI, C., GROSSART, H.-P., MÜHLING, M., JOINT, I. & PASSOW, U. 2011. Dynamics of extracellular enzyme activities in seawater under changed atmospheric pCO2: a mesocosm investigation. *Aquatic Microbial Ecology,* 64**,** 285-298.

ARNOSTI, C., ZIERVOGEL, K., YANG, T. & TESKE, A. 2014. Oil-derived marine aggregates–hot spots of polysaccharide degradation by specialized bacterial communities. *Deep Sea Research Part II: Topical Studies in Oceanography*.

ATLAS, R. M. 1981. Microbial degradation of petroleum hydrocarbons: an environmental perspective. *Microbiological Reviews,* 45**,** 180.

AZAM, F. & HODSON, R. E. 1981. Multiphasic kinetics for D-glucose uptake by assemblages of natural marine bacteria. *Marine Ecology Progress Series***,** 213-222.

AZÚA, I., UNANUE, M., AYO, B., ARTOLOZAGA, I., ARRIETA, J. & IRIBERRI, J. 2003. Influence of organic matter quality in the cleavage of polymers by marine bacterial communities. *Journal of Plankton Research,* 25**,** 1451-1460.

BAINES, S. B. & PACE, M. L. 1991. The production of dissolved organic matter by phytoplankton and its importance to bacteria: patterns across marine and freshwater systems. *Limnology and Oceanography,* 36**,** 1078-1090.

BALTAR, F., ARÍSTEGUI, J., SINTES, E., VAN AKEN, H. M., GASOL, J. M. & HERNDL, G. J. 2009. Prokaryotic extracellular enzymatic activity in relation to biomass production and respiration in the meso-and bathypelagic waters of the (sub) tropical Atlantic. *Environmental microbiology,* 11**,** 1998-2014.

BERGAUER, K., FERNANDEZ-GUERRA, A., GARCIA, J. A. L., SPRENGER, R. R., STEPANAUSKAS, R., PACHIADAKI, M. G., JENSEN, O. N. & HERNDL, G. J. 2018. Organic matter processing by microbial communities throughout the Atlantic water column as revealed by metaproteomics. *Proceedings of the National Academy of Sciences of the United States of America,* 115**,** E400-E408.

BIDDANDA, B. & BENNER, R. 1997. Carbon, nitrogen, and carbohydrate fluxes during the production of particulate and dissolved organic matter by marine phytoplankton. *Limnology and Oceanography,* 42**,** 506-518.

BOOPATHY, R., SHIELDS, S. & NUNNA, S. 2012. Biodegradation of crude oil from the BP oil spill in the marsh sediments of southeast Louisiana, USA. *Applied Biochemistry and Biotechnology,* 167**,** 1560-1568.

CHANTON, J., CHERRIER, J., WILSON, R., SARKODEE-ADOO, J., BOSMAN, S., MICKLE, A. & GRAHAM, W. 2012. Radiocarbon evidence that carbon from the Deepwater Horizon spill entered the planktonic food web of the Gulf of Mexico. *Environmental Research Letters,* 7**,** 045303.

CHRISTIAN, J. R. & KARL, D. M. 1995. Bacterial ectoenzymes in marine waters: activity ratios and temperature responses in three oceanographic provinces. *Limnology and Oceanography,* 40**,** 1042-1049.

CHRÓST, R. J. & OVERBECK, J. 1987. Kinetics of alkaline phosphatase activity and phosphorus availability for phytoplankton and bacterioplankton in lake plu\see (North German Eutrophic Lake). *Microbial ecology,* 13**,** 229-248.

CHRÓST, R. J. & RAI, H. 1993. Ectoenzyme activity and bacterial secondary production in nutrient-impoverished and nutrient-enriched freshwater mesocosms. *Microbial Ecology,* 25**,** 131-150.

DALY, K. L., PASSOW, U., CHANTON, J. & HOLLANDER, D. 2016. Assessing the impacts of oil-associated marine snow formation and sedimentation during and after the Deepwater Horizon oil spill. *Anthropocene,* 13**,** 18-33.

DAVIS, C. E. & MAHAFFEY, C. 2017. Elevated alkaline phosphatase activity in a phosphate-replete environment: Influence of sinking particles. *Limnology and Oceanography,* 62**,** 2389-2403.

DEL GIORGIO, P. A. & COLE, J. J. 1998. Bacterial growth efficiency in natural aquatic systems. *Annual Review of Ecology and Systematics,* 29**,** 503-541.

DOYLE, S. M., WHITAKER, E. A., DE PASCUALE, V., WADE, T. L., KNAP, A. H., SANTSCHI, P. H., QUIGG, A. & SYLVAN, J. B. 2018. Rapid Formation of Microbe-Oil Aggregates and Changes in Community Composition in Coastal Surface Water Following Exposure to Oil and the Dispersant Corexit. *Frontiers in microbiology,* 9**,** 689.

EDWARDS, B. R., REDDY, C. M., CAMILLI, R., CARMICHAEL, C. A., LONGNECKER, K. & VAN MOOY, B. A. 2011. Rapid microbial respiration of oil from the Deepwater Horizon spill in offshore surface waters of the Gulf of Mexico. *Environmental Research Letters,* 6**,** 035301.

FABIANO, M. & DANOVARO, R. 1998. Enzymatic activity, bacterial distribution, and organic matter composition in sediments of the Ross Sea (Antarctica). *Applied and Environmental Microbiology,* 64**,** 3838-3845.

GARCÍA, M. T., CAMPOS, E., MARSAL, A. & RIBOSA, I. 2009. Biodegradability and toxicity of sulphonate-based surfactants in aerobic and anaerobic aquatic environments. *Water Research,* 43**,** 295-302.

HASTINGS, D., SCHWING, P., BROOKS, G., LARSON, R., MORFORD, J., ROEDER, T., QUINN, K., BARTLETT, T., ROMERO, I. & HOLLANDER, D. 2014. Changes in sediment redox conditions following the BP DWH blowout event. *Deep Sea Research Part II: Topical Studies in Oceanography*.

HOPPE, H.-G. 1991. Microbial extracellular enzyme activity: a new key parameter in aquatic ecology. *Microbial enzymes in aquatic environments.* Springer.

HOPPE, H.-G., KIM, S.-J. & GOCKE, K. 1988. Microbial decomposition in aquatic environments: combined process of extracellular enzyme activity and substrate uptake. *Applied and Environmental microbiology,* 54**,** 784-790.

HU, P., DUBINSKY, E. A., PROBST, A. J., WANG, J., SIEBER, C. M., TOM, L. M., GARDINALI, P. R., BANFIELD, J. F., ATLAS, R. M. & ANDERSEN, G. L. 2017. Simulation of Deepwater Horizon oil plume reveals substrate specialization within a complex community of hydrocarbon degraders. *Proceedings of the National Academy of Sciences***,** 201703424.

JOYE, S. B., MACDONALD, I. R., LEIFER, I. & ASPER, V. 2011. Magnitude and oxidation potential of hydrocarbon gases released from the BP oil well blowout. *Nature Geoscience,* 4**,** 160-164.

KAWASAKI, N. & BENNER, R. 2006. Bacterial release of dissolved organic matter during cell growth and decline: molecular origin and composition. *Limnology and Oceanography,* 51**,** 2170-2180.

KIM, S.-J., KWEON, O., SUTHERLAND, J. B., KIM, H.-L., JONES, R. C., BURBACK, B. L., GRAVES, S. W., PSURNY, E. & CERNIGLIA, C. E. 2015. Dynamic response of Mycobacterium vanbaalenii PYR-1 to BP Deepwater Horizon crude oil. *Applied and Environmental Microbiology,* 81**,** 4263-4276.

KLEINDIENST, S., SEIDEL, M., ZIERVOGEL, K., GRIM, S., LOFTIS, K., HARRISON, S., MALKIN, S. Y., PERKINS, M. J., FIELD, J. & SOGIN, M. L. 2015. Chemical dispersants can suppress the activity of natural oil-degrading microorganisms. *Proceedings of the National Academy of Sciences,* 112**,** 14900-14905.

LANCELOT, C. 1979. Gross excretion rates of natural marine phytoplankton and heterotrophic uptake of excreted products in the southern North Sea, as determined by short-term kinetics. *Marine Ecology Progress Series***,** 179-186.

LIU, Z., LIU, J., ZHU, Q. & WU, W. 2012. The weathering of oil after the Deepwater Horizon oil spill: insights from the chemical composition of the oil from the sea surface, salt marshes and sediments. *Environmental Research Letters,* 7**,** 035302.

MARTINEZ, J. & AZAM, F. 1993. Periplasmic aminopeptidase and alkaline phosphatase activities in a marine bacterium: implications for substrate processing in the sea. *Marine Ecology Progress Series***,** 89-97.

MARTINEZ, J., SMITH, D. C., STEWARD, G. F. & AZAM, F. 1996. Variability in ectohydrolytic enzyme activities of pelagic marine bacteria and its significance for substrate processing in the sea. *Aquatic Microbial Ecology,* 10**,** 223-230.

MARX, M.-C., KANDELER, E., WOOD, M., WERMBTER, N. & JARVIS, S. 2005. Exploring the enzymatic landscape: distribution and kinetics of hydrolytic enzymes in soil particle-size fractions. *Soil Biology and Biochemistry,* 37**,** 35-48.

MCNUTT, M. K., CAMILLI, R., CRONE, T. J., GUTHRIE, G. D., HSIEH, P. A., RYERSON, T. B., SAVAS, O. & SHAFFER, F. 2012. Review of flow rate estimates of the Deepwater Horizon oil spill. *Proceedings of the National Academy of Sciences,* 109**,** 20260-20267.

MEYER-REIL, L.-A. 1987. Seasonal and spatial distribution of extracellular enzymatic activities and microbial incorporation of dissolved organic substrates in marine sediments. *Applied and Environmental Microbiology,* 53**,** 1748-1755.

MIRALLES, G., NÉRINI, D., MANTÉ, C., ACQUAVIVA, M., DOUMENQ, P., MICHOTEY, V., NAZARET, S., BERTRAND, J. C. & CUNY, P. 2007. Effects of spilled oil on bacterial communities of Mediterranean coastal anoxic sediments chronically subjected to oil hydrocarbon contamination. *Microbial Ecology,* 54**,** 646-661.

MURRAY, A. E., ARNOSTI, C., CHRISTINA, L., GROSSART, H.-P. & PASSOW, U. 2007. Microbial dynamics in autotrophic and heterotrophic seawater mesocosms. II.

Bacterioplankton community structure and hydrolytic enzyme activities. *Aquatic Microbial Ecology,* 49**,** 123-141.

NIE, Y., ZHAO, J.-Y., TANG, Y.-Q., GUO, P., YANG, Y., WU, X.-L. & ZHAO, F. 2016. Species Divergence vs. Functional Convergence Characterizes Crude Oil Microbial Community Assembly. *Frontiers in Microbiology,* 7.

PALLARDY, R. 2015. Deepwater Horizon oil spill of 2010. *Encyclopaedia Britannica Inc.*

PASSOW, U., ZIERVOGEL, K., ASPER, V. & DIERCKS, A. 2012. Marine snow formation in the aftermath of the Deepwater Horizon oil spill in the Gulf of Mexico. *Environmental Research Letters,* 7**,** 035301.

PATTON, J. S., RIGLER, M. W., BOEHM, P. D. & FIEST, D. L. 1981. Ixtoc 1 oil spill: flaking of surface mousse in the Gulf of Mexico. *Nature,* 290**,** 235-238.

QUIGG, A., PASSOW, U., CHIN, W. C., XU, C., DOYLE, S., BRETHERTON, L., KAMALANATHAN, M., WILLIAMS, A. K., SYLVAN, J. B. & FINKEL, Z. V. 2016. The role of microbial exopolymers in determining the fate of oil and chemical dispersants in the ocean. *Limnology and Oceanography Letters,* 1**,** 3-26.

RITZ, C., STREBIG, J. C. & RITZ, M. C. 2016. Package 'drc'.

ROMERO, I. C., SCHWING, P. T., BROOKS, G. R., LARSON, R. A., HASTINGS, D. W., ELLIS, G., GODDARD, E. A. & HOLLANDER, D. J. 2015. Hydrocarbons in deep-sea sediments following the 2010 Deepwater Horizon blowout in the northeast Gulf of Mexico. *PloS One,* 10**,** e0128371.

SEBASTIÁN, M., ARÍSTEGUI, J., MONTERO, M. F., ESCANEZ, J. & NIELL, F. X. 2004a. Alkaline phosphatase activity and its relationship to inorganic phosphorus in the transition zone of the North-western African upwelling system. *Progress in Oceanography,* 62**,** 131-150.

SEBASTIÁN, M., ARÍSTEGUI, J., MONTERO, M. F. & NIELL, F. X. 2004b. Kinetics of alkaline phosphatase activity, and effect of phosphate enrichment: a case study in the NW African upwelling region. *Marine Ecology Progress Series,* 270**,** 1-13.

SEIDEL, M., KLEINDIENST, S., DITTMAR, T., JOYE, S. B. & MEDEIROS, P. M. 2016. Biodegradation of crude oil and dispersants in deep seawater from the Gulf of Mexico:

Insights from ultra-high resolution mass spectrometry. *Deep Sea Research Part II: Topical Studies in Oceanography,* 129**,** 108-118.

SHILLER, A. M. & JOUNG, D. 2012. Nutrient depletion as a proxy for microbial growth in Deepwater Horizon subsurface oil/gas plumes. *Environmental Research Letters,* 7**,** 045301.

SILLIMAN, B. R., VAN DE KOPPEL, J., MCCOY, M. W., DILLER, J., KASOZI, G. N., EARL, K., ADAMS, P. N. & ZIMMERMAN, A. R. 2012. Degradation and resilience in Louisiana salt marshes after the BP–Deepwater Horizon oil spill. *Proceedings of the National Academy of Sciences,* 109**,** 11234-11239.

SINSABAUGH, R. L. & FOLLSTAD SHAH, J. J. 2012. Ecoenzymatic stoichiometry and ecological theory. *Annual Review of Ecology, Evolution, and Systematics,* 43**,** 313-343.

SMITH, D. C., SIMON, M., ALLDREDGE, A. L. & AZAM, F. 1992. Intense hydrolytic enzyme activity on marine aggregates and implications for rapid particle dissolution. *Nature,* 359**,** 139-142.

STEEN, A. D., VAZIN, J. P., HAGEN, S. M., MULLIGAN, K. H. & WILHELM, S. W. 2015. Substrate specificity of aquatic extracellular peptidases assessed by competitive inhibition assays using synthetic substrates. *Aquatic Microbial Ecology,* 75**,** 271-281.

SYLVAN, J. B., DORTCH, Q., NELSON, D. M., MAIER BROWN, A. F., MORRISON, W. & AMMERMAN, J. W. 2006. Phosphorus limits phytoplankton growth on the Louisiana shelf during the period of hypoxia formation. *Environmental Science & Technology,* 40**,** 7548-7553.

TURNER, R. E., MCCLENACHAN, G. & TWEEL, A. W. 2016. Islands in the oil: Quantifying salt marsh shoreline erosion after the Deepwater Horizon oiling. *Marine pollution bulletin,* 110**,** 316-323.

VAN WAMBEKE, F., PFREUNDT, U., BARANI, A., BERTHELOT, H., MOUTIN, T., RODIER, M., HESS, W. R. & BONNET, S. 2016. Heterotrophic bacterial production and metabolic balance during the VAHINE mesocosm experiment in the New Caledonia lagoon. *Biogeosciences,* 13**,** 3187-3202.

VETTER, Y. & DEMING, J. 1999. Growth rates of marine bacterial isolates on particulate organic substrates solubilized by freely released extracellular enzymes. *Microbial Ecology,* 37**,** 86-94.

WADE, T. L., SERICANO, J. L., SWEET, S. T., KNAP, A. H. & GUINASSO, N. L. 2016. Spatial and temporal distribution of water column total polycyclic aromatic hydrocarbons (PAH) and total petroleum hydrocarbons (TPH) from the Deepwater Horizon (Macondo) incident. *Marine Pollution Bulletin,* 103**,** 286-293.

WADE, T. L., SWEET, S. T., SERICANO, J. L., GUINASSO, N. L., DIERCKS, A. R. R., HIGHSMITH, R. C., ASPER, V. L., JOUNG, D. D., SHILLER, A. M. & LOHRENZ, S. E. 2011. Analyses of water samples from the Deepwater Horizon oil spill: Documentation of the subsurface plume. *Monitoring and Modeling the deepwater horizon oil spill: a record-breaking enterprise***,** 77-82.

WALKER, C. B., DE LA TORRE, J. R., KLOTZ, M. G., URAKAWA, H., PINEL, N., ARP, D. J., BROCHIER-ARMANET, C., CHAIN, P. S. G., CHAN, P. P., GOLLABGIR, A., HEMP, J., HÜGLER, M., KARR, E. A., KÖNNEKE, M., SHIN, M., LAWTON, T. J., LOWE, T., MARTENS-HABBENA, W., SAYAVEDRA-SOTO, L. A., LANG, D., SIEVERT, S. M., ROSENZWEIG, A. C., MANNING, G. & STAHL, D. A. 2010. Nitrosopumilus maritimus genome reveals unique mechanisms for nitrification and autotrophy in globally distributed marine crenarchaea. *Proceedings of the National Academy of Sciences,* 107**,** 8818-8823.

WANG, J., SANDOVAL, K., DING, Y., STOECKEL, D., MINARD-SMITH, A., ANDERSEN, G., DUBINSKY, E. A., ATLAS, R. & GARDINALI, P. 2016. Biodegradation of dispersed Macondo crude oil by indigenous Gulf of Mexico microbial communities. *Science of the Total Environment,* 557**,** 453-468.

WEISS, M., ABELE, U., WECKESSER, J., WELTE, W. U., SCHILTZ, E. & SCHULZ, G. 1991. Molecular architecture and electrostatic properties of a bacterial porin. *Science,* 254**,** 1627-1630.

YAN, B., PASSOW, U., CHANTON, J. P., NÖTHIG, E.-M., ASPER, V., SWEET, J., PITIRANGGON, M., DIERCKS, A. & PAK, D. 2016. Sustained deposition of

contaminants from the Deepwater Horizon spill. *Proceedings of the National Academy of Sciences***,** 201513156.

ZIERVOGEL, K. & ARNOSTI, C. 2016. Enhanced protein and carbohydrate hydrolyses in plume-associated deepwaters initially sampled during the early stages of the Deepwater Horizon oil spill. *Deep Sea Research Part II: Topical Studies in Oceanography,* 129**,** 368-373.

ZIERVOGEL, K., D'SOUZA, N., SWEET, J., YAN, B. & PASSOW, U. 2014. Natural oil slicks fuel surface water microbial activities in the northern Gulf of Mexico. *Frontiers in Microbiology,* 5**,** 10.

ZIERVOGEL, K., MCKAY, L., RHODES, B., OSBURN, C. L., DICKSON-BROWN, J., ARNOSTI, C. & TESKE, A. 2012. Microbial activities and dissolved organic matter dynamics in oil-contaminated surface seawater from the Deepwater Horizon oil spill site. *PloS One,* 7**,** e34816.

ZIMMERMAN, A. E., MARTINY, A. C. & ALLISON, S. D. 2013. Microdiversity of extracellular enzyme genes among sequenced prokaryotic genomes. *The ISME Journal,* 7**,** 1187-1199.